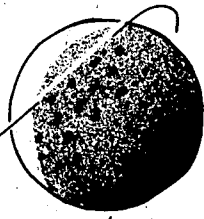


148



**CALCULATION OF TRAJECTORIES USING CONSTANT
AND SLOWLY VARYING FUNCTIONS**

BY
BOBBY K. CULPEPPER

AMRL 1045

DECEMBER, 1971

(ROAD)

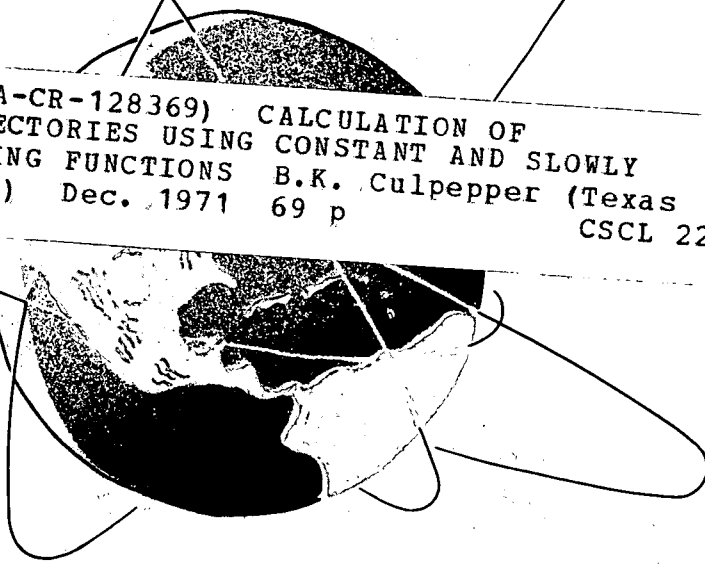
(NASA-CR-128369) CALCULATION OF
TRAJECTORIES USING CONSTANT AND SLOWLY
VARYING FUNCTIONS B.K. Culpepper (Texas
Univ.) Dec. 1971 69 p

N72-33778

CSCL 22C

G3/30

Unclas
16505



APPLIED MECHANICS RESEARCH LABORATORY
THE UNIVERSITY OF TEXAS AT AUSTIN AUSTIN, TEXAS

CALCULATION OF TRAJECTORIES USING CONSTANT AND SLOWLY VARYING FUNCTIONS

Bobby K. Culpepper
The University of Texas at Austin
Austin, Texas

AMRL 1045
December 1971

Applied Mechanics Research Laboratory
The University of Texas at Austin
Austin, Texas

I

This report was prepared under

Contract No. NGL-44-012-008

for the

National Aeronautics and Space Administration
Headquarters

by the

Applied Mechanics Research Laboratory
The University of Texas at Austin
Austin, Texas

under the direction of

Paul E. Russell
Assistant Professor

/

PREFACE

Since the problem of two bodies is the only problem in astrodynamics with a known solution for arbitrary initial conditions, it has been used in an approximate solution to the restricted problem of three bodies in the form of patched conic orbits. Since the development of the patched conic technique, several methods of approximating the solution to the restricted problem of three bodies have been presented, but none of them utilize full knowledge of the known integrals for the exact motion. It is believed that a method that uses knowledge of the known functions of the motion and is conceptually simple would be quite useful for studies of future space missions.

This study presents a method of calculating trajectories for the restricted problem of three bodies using conic motion that is frequently corrected in position and velocity. The correction in position and velocity is calculated using knowledge of the existing integrals or slowly-varying functions of the motion. This method is easily described. Assume that the trajectory has just been corrected. The motion to the next correction point and the correction there will be described. The independent variable is the magnitude of the radius vector. A change in the independent variable Δr is chosen and the trajectory is conically advanced through the interval Δr . Since the value of the function of the motion evaluated on the conic trajectory is not the same as the value predicted for the exact motion, position and velocity corrections are applied to the conic trajectory so that the value of the function will be the same as the predicted value. The process is repeated until the terminal conditions are reached.

The results of this method are compared with numerically integrated trajectories. This method is qualitatively compared with other methods of

solution for the restricted problem of three bodies.

Sincere appreciation is expressed to Dr. P. E. Russell for serving as advisor and for his encouragement and guidance during the author's course of study at The University of Texas at Austin. Thanks, also, are extended to Dr. B. D. Tapley, Dr. Victor Szebehely and Dr. W. T. Fowler for serving on the supervising committee.

A special thanks is extended to Dr. W. E. Williamson, Dr. D. S. Ingram, Mr. R. W. Greene, and Mr. James R. Elk of NASA's Manned Spacecraft Center for their encouragement throughout the investigation. The author, also, expresses his appreciation to Mr. and Mrs. John Burchard, Dr. and Mrs. R. V. Murray, and many other friends at the Allandale Baptist Church of Austin. Sincere gratitude is expressed to the author's wife, Norma, his son, Scott, and immediate family for their support and encouragement throughout his education. The author appreciates Mrs. Hope Ince and Mrs. Mollie Schluter for typing this manuscript. In addition, the author is pleased to acknowledge the National Aeronautics and Space Administration under Grants NGR 44-012-0132 and NGR 44-012-0136, and the Bureau of Engineering Research for support during the course of this investigation.

Bobby K. Culpepper

September 1971
Austin, Texas

ABSTRACT

This report presents a method of calculating trajectories for the restricted problem of three bodies which utilizes conic propagation of the state vector with frequent correction of position and velocity by means of a constant or slowly-varying function. This fast and accurate method of calculating trajectories has been applied to the planar circular restricted problem of three bodies, the planar elliptic restricted problem of three bodies, and the ephemeral restricted problem of three bodies. Two methods (the "refined" method and the "straight-forward" method) of determining the direction of the position correction (\bar{n}_c) are presented for the circular restricted problem and the elliptic restricted problem of three bodies. Only the "straight-forward" method is used with the ephemeral restricted problem of three bodies. The Earth, the Moon and a space vehicle comprise the restricted three body model that is used. Earth-to-Moon trajectories with perilune altitudes varying from 59 to 4551 nautical miles are calculated and compared at perilune with numerically integrated and patched conic trajectories. The results, as compared to the numerically integrated trajectories, are within 0.2% in position and velocity vector magnitude (relative to the Moon) for the "straight-forward" and the "refined" choices of the position correction direction (\bar{n}_c).

A detailed discussion of the two methods of choosing \bar{n}_c is presented. A qualitative comparison between this method and other methods of calculating trajectories for the restricted problem of three bodies is also presented.

PRECEDING PAGE BLANK NOT FILMED

TABLE OF CONTENTS

	Page
PREFACE	ii
ABSTRACT	iv
LIST OF FIGURES	viii
LIST OF TABLES	ix
NOMENCLATURE	x
CHAPTER 1 - INTRODUCTION	1
1.1 GENERAL BACKGROUND	1
1.2 RESTRICTED PROBLEM OF THREE BODIES	1
1.2.1 PLANAR CIRCULAR RESTRICTED PROBLEM OF THREE BODIES	2
1.2.2 PLANAR ELLIPTIC RESTRICTED PROBLEM OF THREE BODIES	2
1.2.3 EPHEMERAL RESTRICTED PROBLEM OF THREE BODIES	2
1.3 APPROXIMATE SOLUTIONS	3
1.4 MOTIVATION	6
CHAPTER 2 - DESCRIPTION OF METHOD	8
2.1 ASSUMPTIONS	8
2.2 DEVELOPMENT OF GENERAL EQUATIONS OF MOTION	9
2.3 METHOD OF CALCULATION OF TRAJECTORIES	12
CHAPTER 3 - CIRCULAR RESTRICTED PROBLEM OF THREE BODIES	17
3.1 EQUATIONS FOR THE CIRCULAR RESTRICTED PROBLEM OF THREE BODIES	17
3.2 VELOCITY CORRECTION DIRECTION \bar{n}_p	18
3.3 POSITION CORRECTION DIRECTION \bar{n}_c	19
3.4 NUMERICAL RESULTS FOR "REFINED" CHOICE OF \bar{n}_c	20
3.5 NUMERICAL RESULTS FOR THE "STRAIGHT-FORWARD" CHOICE OF \bar{n}_c	25

Preceding page blank

	Page
CHAPTER 4 - ELLIPTIC RESTRICTED PROBLEM OF THREE BODIES	28
4.1 EQUATION FOR THE ELLIPTIC RESTRICTED PROBLEM OF THREE BODIES . . .	28
4.2 NUMERICAL RESULTS FOR "REFINED" AND "STRAIGHT-FORWARD" CHOICE OF \bar{n}_c	30
CHAPTER 5 - EPHEMERAL RESTRICTED PROBLEM OF THREE BODIES	35
5.1 EQUATION FOR THE EPHEMERAL RESTRICTED PROBLEM OF THREE BODIES .	35
5.2 VELOCITY CORRECTION DIRECTION \bar{n}_p	36
5.3 POSITION CORRECTION DIRECTION \bar{n}_c	37
5.4 NUMERICAL RESULTS FOR THE EPHEMERAL RESTRICTED PROBLEM OF THREE BODIES	37
CHAPTER 6 - DISCUSSION OF CHOICE OF CORRECTION DIRECTION	45
6.1 BACKGROUND HISTORY	45
6.2 LOGICAL STEPS THAT LED TO THE CHOICE OF \bar{n}_c	45
CHAPTER 7 - COMPARISONS, CONCLUSION, AND RECOMMENDATIONS	48
7.1 SUMMARY	48
7.2 COMPARISON OF METHODS	48
7.3 CONCLUSIONS	50
7.4 RECOMMENDATIONS FOR FUTURE STUDY	52
BIBLIOGRAPHY	53
VITA	

LIST OF FIGURES

Figure		Page
1.1	Diagram for the Restricted Problem of Three Bodies	1
1.2	Patched Conic Geometry for Primary 1 to Primary 2 Trajectories	3
2.1	Configuration of the Earth, the Moon, and the Space Vehicle	8
2.2	Diagram for the Restricted Problem of Three Bodies	9
3.1	The Variation of Mean Anomaly and Position Vector Magnitude .	19
3.2	Polar Coordinate Systems	19
3.3	The Variation of ϕ With Perilune Altitude for the Circular Restricted Problem of Three Bodies	20
4.1	The Variation of ϕ With Perilune Altitude for the Elliptic Restricted Problem of Three Bodies	30
5.1	Cylindrical Coordinates Used in the Ephemeral Restricted Problem of Three Bodies	39

LIST OF TABLES

Table		Page
1	Numerical Results at Perilune for "Refined" Choice of \bar{n}_c for the Circular Restricted Problem of Three Bodies	23
2	Numerical Results at Perilune for "Straight-Forward" Choice of \bar{n}_c for the Circular Restricted Problem of Three Bodies	26
3	Numerical Results at Perilune for Jacobi-1 "Refined" Choice of \bar{n}_c and Jacobi-2 "Straight-Forward" Choice of \bar{n}_c for the Elliptic Restricted Problem of Three Bodies	32
4	Numerical Results at Perilune for "Straight-Forward" Choice of \bar{n}_c for the Ephemeral Restricted Problem of Three Bodies	41

NOMENCLATURE

The following list presents all significant symbols and abbreviations used in the main body of the text. Each symbol is accompanied by a brief description and the number of the equation where the symbol is introduced.

Vectors:

\bar{A}	vector ($\bar{A} = \frac{0}{r}$) used in Equation (2.36)
\bar{a}	average perturbing acceleration (2.33a)
\bar{B}	vector used in Equation (2.37)
$\begin{bmatrix} \bar{e}_r \\ \bar{e}_\alpha \end{bmatrix}$	unit vectors relative to the space vehicle (3.7)
$\begin{bmatrix} \bar{e}_x \\ \bar{e}_y \\ \bar{e}_z \end{bmatrix}$	unit vectors describing primary two relative to primary one (2.13)
\bar{h}	angular momentum of massless particle (2.18)
\bar{n}_c	unit vector in position correction direction (2.29)
\bar{n}_p	unit vector in the velocity correction direction (2.23)
\bar{R}_1	position vector of primary one relative to CM (2.3)
\bar{R}_2	position vector of primary two relative to CM (2.3)
$\bar{R}_{2/1}$	position vector of primary two relative to primary one
\bar{r}	position vector of massless particle relative to CM (2.1)
\bar{r}_1	position vector of massless particle relative to primary one (2.1)

\bar{r}_2	position vector of massless particle relative to primary two (2.1)
$\Delta\bar{R}$	change of position vector (7.2)
$\Delta\bar{V}$	change of velocity vector (7.1)
$\delta\bar{r}$	position vector correction (2.28)
$\dot{\delta}\bar{r}$	velocity vector correction (2.28)
$\bar{\omega}$	angular velocity of primaries about CM (2.10)

Scalars:

$E_{2/1}$	eccentric anomaly of primary two relative to primary one (4.2)
$e_{2/1}$	eccentricity of primary two relative to primary one (4.2)
$\dot{f}_{2/1}$	angular velocity of primary two relative to primary one (4.3)
G	universal gravitational constant in Section (3.4)
J	Jacobi function (2.16)
\dot{J}	rate of change of Jacobi function (2.17)
J_c	J evaluated on the conic trajectory (2.27)
m_1	dimensional mass of primary one (2.2)
m_2	dimensional mass of primary two (2.2)
R_1	projection of r_1 onto the Earth-Moon plane for the ephemerical restricted problem of three bodies
R_2	projection of r_2 onto the Earth-Moon plane (5.7)
r	magnitude $ \bar{r} $ (2.1)
r_1	magnitude $ \bar{r}_1 $ (2.1)
r_2	magnitude $ \bar{r}_2 $ (2.1)

r_o	initial value of r (2.25)
r_f	final value of r (2.25)
Δr	increment in r (2.25)
Δr_o	initial increment in Δr (2.25)
Δr_f	final increment in Δr (2.25)
Δt	increment in time $(t_2 - t_1)$ (2.26a)
δt	time correction (2.30)
δr	magnitude $ \delta \bar{r} $ (2.29)
$\dot{\delta r}$	magnitude $ \dot{\delta \bar{r}} $ (2.29)
α	angle from \bar{e}_x to \bar{e}_r [Figure (3.2)]
$\dot{\theta}_i$	($i = 1,2$) angular velocity of \bar{r}_i
μ	mass ratio-parameter (2.2)
σ	variable = ± 1 (3.11)
ϕ	angle between \bar{e}_r and \bar{n}_c (3.7)
ω	magnitude $ \bar{\omega} $

Subscripts:

f	indicates final value
i	indicates 1 or 2
o	indicates initial value
p	indicates perturbing acceleration direction
x	referenced to x direction
y	referenced to y direction
z	referenced to z direction

Miscellaneous Symbols:

$(\dot{\quad})$ indicates $\frac{d}{dt}(\quad)$

$(\overset{\circ}{\quad})$ indicates $\frac{d}{dt}(\quad)$ within the rotating coordinate system

Abbreviations: Numbers to the side represent Sections where they first appear.

CM center of mass (2.2)

er Earth radii (3.4)

fps feet/second (3.4)

hr hour (3.4)

min minute

n. mi nautical mile (3.4)

rad radians (Table 1)

sec second (3.4)

CHAPTER 1

INTRODUCTION

1.1 General Background

Since the problem of two bodies is the only problem in astrodynamics with a known solution for arbitrary initial conditions, it has been used extensively as a model of the problem of planet-orbiting satellites. The solution to the problem of two bodies is also a good approximation to the motion of the planets relative to the sun. However, it is not a good approximation for Earth-Moon or interplanetary trajectories, because it cannot include multiple force centers. This led to the use of the restricted* problem of three bodies as a mathematical model for Earth-Moon trajectories and successive portions of interplanetary trajectories.

1.2 Restricted Problem of Three Bodies

The restricted problem of three bodies in this study is the motion of a massless particle (space vehicle) in the vicinity of two massive primaries (see Figure 1.1). The unit base vectors \bar{e}_x and \bar{e}_y are in the plane

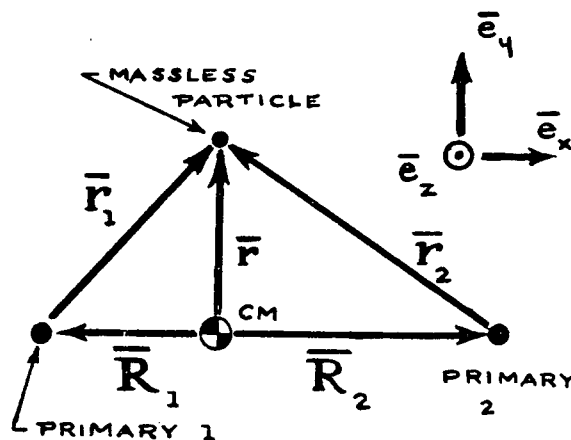


Figure 1.1 Diagram for the Restricted Problem of Three Bodies

*Restricted in the sense that the mass of the third body is small enough that it does not affect the motion of the two primaries.

containing the motion of the two primaries relative to the center of mass (CM) and \bar{e}_z is the unit vector perpendicular to that plane.

1.2.1 Planar Circular Restricted Problem of Three Bodies

The circular restricted problem of three bodies is the configuration where the two primaries are in circular orbits about the CM and the motion of the particle is in the plane of motion of the two primaries.

1.2.2 Planar Elliptic Restricted Problem of Three Bodies

The elliptic restricted problem of three bodies is the system where the two primaries are in elliptic orbits relative to the CM. The motion of the particle is again in the plane of the motion of the two primaries.

1.2.3 Ephemeral Restricted Problem of Three Bodies

The ephemeral restricted problem of three bodies is the three-dimensional motion of the massless particle, where the position and velocities of the primaries (the Earth and the Moon) are obtained from available ephemeris information. Such ephemeris information is available in readily accessible form for computer use on the JPL ephemeris tape^[6].*

For arbitrary initial conditions there are no known analytic solutions to any of the above mentioned problems. Since the restricted problem of three bodies is a representative mathematical model of the Earth-Moon space vehicle system and of successive parts of interplanetary trajectories, it is desirable to have a fast, accurate solution from the standpoint of guidance and trajectory analyses. This solution can be used to determine parameter sensitivity and guidance sensitivity for several trajectories with little

*Numbers appearing in the text as superscripts indicate references listed in the Bibliography.

computer time expense. To perform a similar analysis using a numerical integration technique would be very expensive in terms of computer time.

1.3 Approximate Solutions

The patched conic, introduced by Egorov^[7] in 1958, was one of the first approximate solutions to the restricted problem of three bodies. The patched conic for the restricted problem of three bodies consists of two conic segments, the conic of a particle about primary one without the perturbations of primary two and the conic of the same particle about primary two without primary one perturbations, which are joined at a point in space to produce the composite trajectory. The joining point in space is taken to lie on the surface of a nearly spherical surface, centered at primary two, which is called the Mean Surface of Influence and is discussed in Ref. [8] (see Figure 1.2).

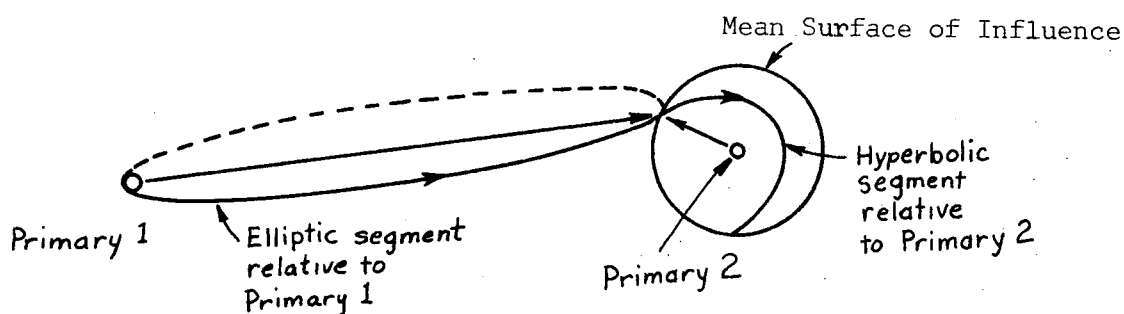


Figure 1.2 Patched Conic Geometry for Primary 1 to Primary 2 Trajectories

Some of the disadvantages of the patched-conic are:

1. it produces large errors for trajectories that have long transit times,
2. it is sensitive to the choice of the magnitude of the mean surface of influence, and
3. it has no means of including the effect of the perturbing body.

Its advantages are:

1. it is very fast computationally
2. it provides reasonable velocity requirements if the initial and final position vectors are given.

The method of matched asymptotic expansions^[11,12,13] is another method of approximating the trajectory of a particle in the presence of two primaries. The initial difficulty of the matched asymptotic expansion is the algebra and computer program check out required to obtain suitable results. Until later refinements were applied to the method^[14], the computer time required to obtain a solution is almost as large as the time required to obtain a numerically integrated trajectory.

During the period of time from 1963 to 1966 much work was done at NASA and TRW Systems to improve the patched-conic by applying a velocity correction at the patch point^[27,28]. The velocity correction being calculated from knowledge of the "Jacobian Function" for the restricted problem of three bodies. This method was an improvement to the patched conic, but was not sufficient for all cases.

During the period of time from 1967 to 1969 the Hybrid Patched-Conic Technique was developed by Escobal, et al.^[9] At first appearance it seemed that the Hybrid Patched Conic Technique was accurate and fast enough to meet the needs of NASA and industry at the time. The disadvantages to the Hybrid

Patched Conic Technique are that it requires a patched conic solution for a reference trajectory, and its accuracy is limited if the perilune altitude is large (e.g., greater than 3000 n.mi.).

In 1969 this investigation was initiated using knowledge of the "Jacobian Condition" and the "angular Momentum condition" to make corrections at several points along the trajectory to see if this would not produce a quickly-calculated trajectory that was sufficiently accurate, as compared to a numerically integrated solution. It was later determined that the angular momentum correction was not accurate enough to help improve the accuracy.

After the present investigation was initiated, it was learned that several individuals at TRW Systems at Houston were working on the same type of problems but with quite different approaches. They developed the multi-conic method^[4] and the pseudo-conic method^[31].

The multi-conic method uses two-body motion as the basic propagation technique. Gravitational effects are accounted for by assuming that each perturbing body causes independent two-body motion. The effects are then summed along the trajectory. The procedure does involve a retracing step and using a zero gravity step. Thus, the method is more complicated than the "Jacobian" correction method presented here.

The pseudo-conic method also uses conic motion as method of propagation, but it continues on past the mean surface of influence along a trajectory that is regarded as a pseudostate. Then it propagates from the mean surface of influence to the desired final time. The pseudo-conic does reduce the patched conic error considerably, but it does not seem to be as accurate as the multi-conic method.

An "integral hypersurface" technique^[1,15,16,17] has been used by Nacozy^[17] to constrain the numerically integrated solution to remain on the

integral surfaces. A similar technique has been used iteratively by Miller^[15] in a gravitational n-body integration to control the usual ten first integrals of motion. Miller^[16] also used the first ten integrals of the equations of motion as controls for n-body integration. In a comparison of a corrected solution of the system with a similar, uncorrected solution, he finds that the two solutions diverge from each other - indicating the instability of the gravitational system. Aarseth^[1] used a similar integral surfaces technique to correct the integrals, the positions, and the velocities of the computed solution to account for the removal of escaping bodies from the system.

1.4 Motivation

The motivation for the approach taken here is that proper use of the knowledge obtained from the "Jacobian" Function could produce results that are a significant improvement over the results obtained from a patched conic trajectory with much less computer time than is required for numerical integration^[24].

The first step was to apply the theory to the planar circular restricted problem of three bodies.^[23] Since the Jacobian Function is a constant for the circular restricted problem of three bodies, it was felt that it would be best to apply the theory to the circular restricted problem of three bodies before proceeding to the elliptic and ephemeral restricted problem of three bodies. The description of the method and the necessary equations are derived in Chapter 2. The application to and the results obtained from the circular restricted problem of three bodies are presented in Chapter 3. Next, the elliptic restricted problem of three bodies is treated and the results presented in Chapter 4. Last, the ephemeral restricted problem of three bodies application and results are presented in Chapter 5. A detailed discussion of

the choice of the position vector correction direction (\bar{n}_c) and the velocity vector correction direction (\bar{n}_p) is presented in Chapter 6. The summary and conclusions are presented in Chapter 7.

A qualitative comparison of the patched conic, the hybrid patched conic technique, the matched asymptotic expansion technique, the multi-conic, and the pseudo-conic is also presented in Chapter 7.

CHAPTER 2
DESCRIPTION OF METHOD

2.1 Assumptions

If the effects of the gravitational fields of the sun and other planets are neglected, the system containing the Earth, the Moon, and a space vehicle can be approximated as a three-body system (see Figure 2.1).

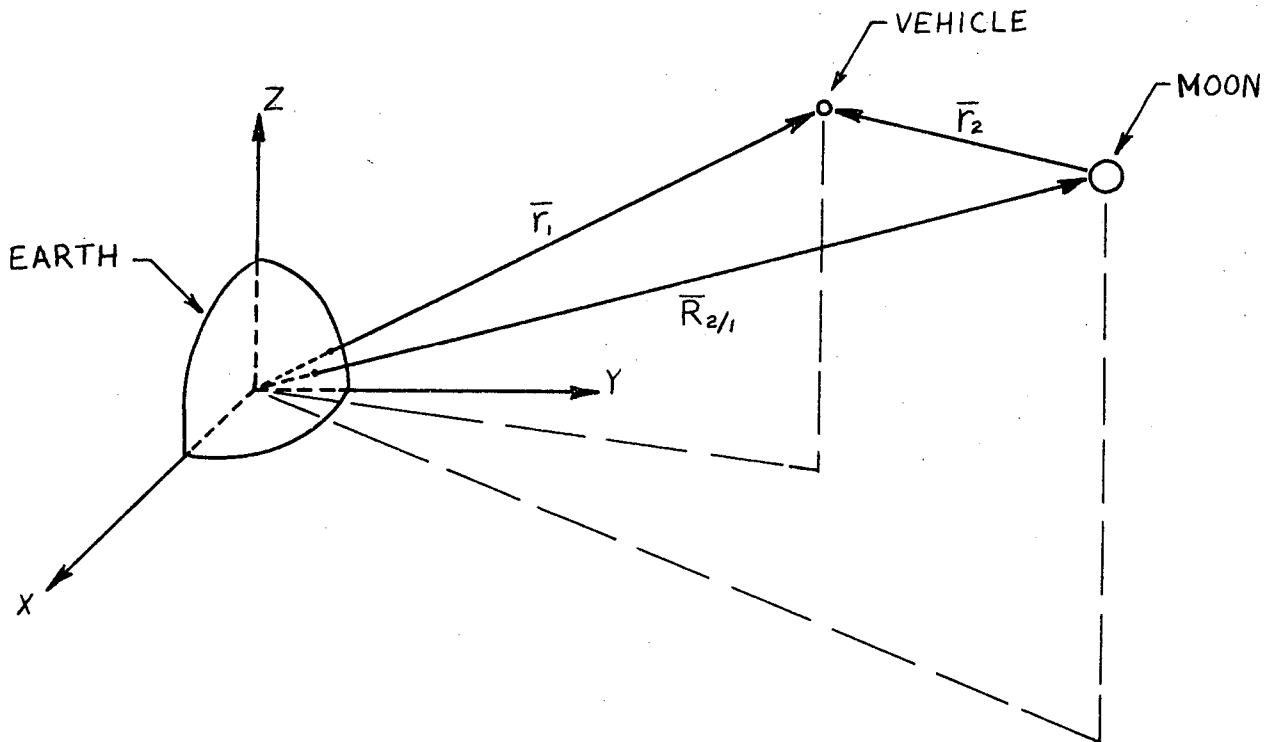


Figure 2.1 Configuration of the Earth, the Moon, and the Space Vehicle.

This can be modeled, as in Figure 2.2, as the restricted problem of three bodies. The restriction is that the space vehicle (or the massless particle) does not affect the motion of the two primaries. The masses of the two primaries are assumed to be spherically symmetric and homogeneous in concentric layers.

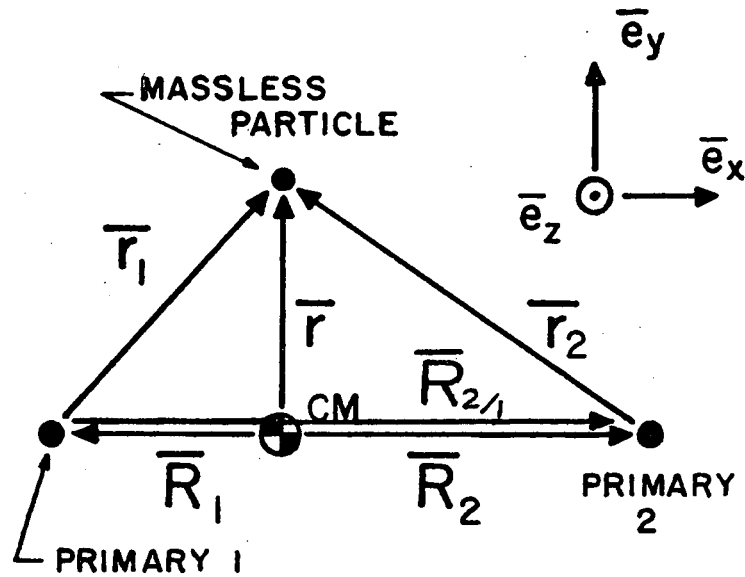


Figure 2.2 Diagram for the Restricted Three-Body Problem (R3BP).

The problem will be formulated in a vectorial notation that can be used for both two- and three-dimensional problems. For the ephemeral restricted problem of three bodies the position and velocities of the primaries (the Earth and the Moon) are obtained from the JPL ephemeris tape^[6].

2.2 Development of the General Equations of Motion

The non-dimensional equation of motion for the massless particle is

$$\ddot{\bar{r}} + (1 - \mu) \frac{\bar{r}_1}{r_1^3} + \mu \frac{\bar{r}_2}{r_2^3} = 0 \quad (2.1)$$

(see Figure 2.2) where μ , the mass ratio-parameter, is

$$\mu = \frac{m_2}{(m_1 + m_2)} \quad (2.2)$$

and m_1 and m_2 are the dimensional masses of the two primaries.

$\ddot{\bar{r}}$ = acceleration of the massless particle relative to the center of mass (CM).

\bar{r} = position vector of the massless particle relative to the CM.

\bar{r}_1 = position vector of the massless particle relative to primary one.

\bar{r}_2 = position vector of the massless particle relative to primary two.

Therefore,

$$\bar{r}_1 = \bar{r} - \bar{R}_1, \quad \bar{r}_2 = \bar{r} - \bar{R}_2 \quad (2.3)$$

$$\ddot{\bar{r}}_1 = \ddot{\bar{r}} - \ddot{\bar{R}}_1, \quad \ddot{\bar{r}}_2 = \ddot{\bar{r}} - \ddot{\bar{R}}_2 \quad (2.4)$$

$$\bar{R}_1 = -\mu \bar{R}_{2/1} \quad (2.5)$$

$$\bar{R}_2 = (1 - \mu) \bar{R}_{2/1} \quad (2.6)$$

$$\bar{R}_{2/1} = \bar{R}_2 - \bar{R}_1 = \bar{e}_x R_{2/1} \quad (2.7)$$

where

$\bar{R}_{2/1}$ = Position vector of Primary two relative to Primary one.

\bar{R}_1 = Position vector of Primary one relative to the CM.

\bar{R}_2 = Position vector of Primary two relative to the CM.

The equations of motion relative to primary one and primary two are, respectively,

$$\ddot{\bar{r}}_1 + (1 - \mu) \frac{\bar{r}_1}{r_1^3} + \mu \left\{ \frac{\bar{r}_2}{r_2^3} + \frac{\bar{R}_{2/1}}{R_{2/1}^3} \right\} = 0 \quad (2.8)$$

and

$$\ddot{\bar{r}}_2 + \mu \frac{\bar{r}_2}{r_2^3} + (1 - \mu) \left\{ \frac{\bar{r}_1}{r_1^3} - \frac{\bar{R}_{2/1}}{R_{2/1}^3} \right\} = 0 \quad (2.9)$$

The velocity $\dot{\bar{r}}$ and acceleration $\ddot{\bar{r}}$ can be written as

$$\dot{\bar{r}} = \dot{\bar{r}}^0 + \bar{\omega} \times \bar{r} \quad (2.10)$$

$$\ddot{\bar{r}} = \ddot{\bar{r}}^0 + \bar{\omega} \times (\bar{\omega} \times \bar{r}) + 2\dot{\bar{\omega}} \times \bar{r} + \dot{\bar{\omega}} \times \bar{r} \quad (2.11)$$

where

$$\dot{\bar{r}} = \frac{d}{dt} (\bar{r}) \quad (2.12a)$$

$$\dot{\bar{r}}^0 \equiv d\bar{r}/dt \text{ with } \bar{e}_x, \bar{e}_y, \bar{e}_z \text{ fixed.} \quad (2.12b)$$

In the cartesian coordinate system indicated by the rotating, unit base vectors $\bar{e}_x, \bar{e}_y, \bar{e}_z,$

$$\bar{r} = x\bar{e}_x + y\bar{e}_y + z\bar{e}_z \quad (2.13)$$

$$\dot{\bar{r}}^0 = \dot{x}\bar{e}_x + \dot{y}\bar{e}_y + \dot{z}\bar{e}_z \quad (2.14)$$

$\bar{\omega} =$ angular velocity of primaries about the CM .

$$= \omega\bar{e}_z \quad (2.15)$$

The Jacobian function for the restricted problem of three bodies and its derivative are^[3,29].

$$J = \frac{1}{2} \dot{\bar{r}}^0 \cdot \dot{\bar{r}}^0 - \frac{1}{2} (\bar{\omega} \times \bar{r}) \cdot (\bar{\omega} \times \bar{r}) - (1 - \mu)/r_1 - \mu/r_2 \quad (2.16)$$

and

$$\dot{J} = -\dot{\bar{\omega}} \cdot \bar{h} + \mu(1 - \mu)\bar{R}_{2/1}^0 \cdot \begin{pmatrix} \bar{r}_1 & \bar{r}_2 \\ r_1^3 & r_2^3 \end{pmatrix} \quad (2.17)$$

where

$$\begin{aligned} \bar{h} &= \text{angular momentum of the massless} \\ &\quad \text{particle relative to the CM .} \\ &= \bar{r} \times \dot{\bar{r}} = \bar{r} \times \dot{\bar{r}}^0 + \bar{\omega} r^2 - \bar{r}(\bar{\omega} \cdot \bar{r}) \end{aligned} \quad (2.18)$$

This assumes that no other forces are acting on the system and

$$\ddot{\bar{R}}_{2/1} + \frac{\bar{R}_{2/1}}{R_{2/1}^3} = 0 \quad (2.19)$$

which implies that

$$\bar{\omega} = \omega \bar{e}_z = (\bar{R}_{2/1} \times \dot{\bar{R}}_{2/1}) / R_{2/1}^2 \quad (2.20)$$

For the case of the circular restricted problem of three bodies it is clear that

$$\dot{\bar{\omega}} \equiv 0 \quad \text{and} \quad \overset{\circ}{\bar{R}}_{2/1} \equiv 0 \quad (2.21)$$

This then leads to the well known Jacobian integral for the circular restricted problem of three bodies (see pp. 16 of Ref. 29). That is,

$$J = \frac{1}{2} \overset{\circ}{\bar{r}} \cdot \overset{\circ}{\bar{r}} - \frac{1}{2} (\bar{\omega} \times \bar{r}) \cdot (\bar{\omega} \times \bar{r}) - (1-\mu)/r_1 - \mu/r_2 = \text{Const.} \quad (2.22)$$

Further details of each of these equations (2.1-2.22) will be discussed as necessary in the remaining Chapters.

It is desirable at this point to discuss the method of application.

2.3 Method of Calculation of Trajectories

Due to its computational simplicity, conic motion has been chosen to be the method of trajectory advancement. The force center is the primary on the same side of the surface of influence as the massless particle (the surface of influence is defined on p. 148 ff of Ref. 8) and the independent variable is the magnitude of the position vector from the force center. This choice of independent variable eliminates the need for iteration involving Kepler's equation.

After the trajectory has been conically advanced over the desired position vector magnitude interval, a correction to the position and velocity

is calculated using the Jacobian function, which is constant or slowly-varying for the exact motion. Slowly-varying functions [Equation (2.17)] must be integrated over the propagation interval.

In the application of this method to the restricted problem of three bodies one scalar (Jacobian) function is involved in the correction procedure. This function is used to correct one velocity vector component and one position vector component. The direction of the velocity component is the approximate direction of the time-averaged perturbing acceleration. The position component's direction is different and is discussed in Chapter 6.

The direction of the perturbing acceleration is obtained from Equations (2.8) and (2.9). For motion relative to primary one the unit vector in the direction of the average perturbing acceleration

$$\bar{n}_p = \frac{- (\bar{R}_{2/1}/R_{2/1}^3 + \bar{r}_2/r_2^3)}{|R_{2/1}/R_{2/1}^3 - \bar{r}_2/r_2^3|} \quad (2.23)$$

where $| \quad |$ indicates the absolute value. For motion relative to primary two this is

$$\bar{n}_p = \frac{- \left(-\bar{R}_{2/1}/R_{2/1}^3 + \bar{r}_1/r_1^3 \right)}{\left| -\bar{R}_{2/1}/R_{2/1}^3 + \bar{r}_1/r_1^3 \right|} \quad (2.24)$$

Further details of the correction direction procedure will be given as necessary in the appropriate sections.

Assume that the trajectory has just been corrected. The motion to the next correction point and the correction there will be described.

The interval of propagation Δr is chosen to vary linearly with r and is calculated by means of the equation.

$$\Delta r = \Delta r_0 + (\Delta r_f - \Delta r_0)(r - r_0)/(r_f - r_0) \quad (2.25)$$

Where r_0 and Δr_0 are initial values and r_f and Δr_f are final values. The state vector is conically propagated to a new state vector at $r + \Delta r$. Due to the choice of independent variable, no iterations are necessary and this is a straightforward procedure.

At the new conically-advanced state, a "conic" Jacobian function and its derivative J_c and \dot{J}_c are calculated. The approximate values of J and \dot{J} at the newly advanced state are predicted using trapezoidal integration. That is,

$$J_2 = J_1 + 0.5(\dot{J}_1 + \dot{J}_2)\Delta t \quad (2.26)$$

where J_2 is the predicted value of J at $r + \Delta r$, J_1 and \dot{J}_1 are the values of J and \dot{J} evaluated at the previous r , and

$$\Delta t = t_2 - t_1 \quad (2.26a)$$

where t_1 is the time associated with the trajectory at r and t_2 is the time associated with the trajectory at $r + \Delta r$. The derivative \dot{J}_2 is \dot{J} evaluated on the conic trajectory at t_2 . Then $J \rightarrow J_2$. Since the exact motion is not conic

$$J_c \neq J \quad (2.27)$$

At this point, correct both velocity and position vectors.

$$\dot{\bar{r}} \rightarrow \dot{\bar{r}} + \delta \dot{\bar{r}} \quad ; \quad \bar{r} \rightarrow \bar{r} + \delta \bar{r} \quad (2.28)$$

and

$$\delta \dot{\bar{r}} = \bar{n}_p \delta r \quad ; \quad \delta \bar{r} = \bar{n}_c \delta r \quad (2.29)$$

The unit vector \bar{n}_p indicates the direction of the velocity correction while

\bar{n}_c indicates the position vector correction direction. These are discussed in Chapter 6.

Note that, since the time correction

$$\delta t \equiv 0 \quad (2.30)$$

the following equations are true:

$$\dot{\delta \bar{r}} = \dot{\delta \bar{r}}_1 = \dot{\delta \bar{r}}_2 \quad ; \quad \delta \bar{r} = \delta \bar{r}_1 = \delta \bar{r}_2 \quad (2.31)$$

The equation for determining $\dot{\delta \bar{r}}$ and $\delta \bar{r}$ is

$$\begin{aligned} & \frac{1}{2} (\overset{o}{\bar{r}} + \overset{o}{\delta \bar{r}}) \cdot (\overset{o}{\bar{r}} + \overset{o}{\delta \bar{r}}) - \frac{1}{2} \overset{o}{\bar{r}} \cdot \overset{o}{\bar{r}} - \frac{1}{2} [\bar{\omega} \times (\bar{r} + \delta \bar{r})] \\ & \cdot [\bar{\omega} \times (\bar{r} + \delta \bar{r})] + \frac{1}{2} (\bar{\omega} \times \bar{r}) \cdot (\bar{\omega} \times \bar{r}) - (1 - \mu)/(r_1 + \delta r_1) \quad (2.32) \\ & + (1 - \mu)/r_1 - \mu/(r_2 + \delta r_2) + \mu/r_2 = J - J_c \end{aligned}$$

Since two scalar quantities are being corrected by means of one scalar function, a relationship between $\dot{\delta \bar{r}}$ and $\delta \bar{r}$ is needed. If \bar{a} is the average perturbing acceleration,

$$\dot{\delta \bar{r}} = \bar{a} \Delta t \quad (2.33a)$$

$$\delta \bar{r} = \frac{1}{2} \bar{a} (\Delta t)^2 = \frac{1}{2} (\dot{\delta \bar{r}}) (\Delta t) \quad (2.33b)$$

where Δt is the time interval corresponding to Δr and is evaluated from Kepler's equation. Ignore the difference between \bar{n}_p and \bar{n}_c (see Chapter 6) and use

$$\delta r = \frac{1}{2} (\dot{\delta r}) (\Delta t) \quad (2.34)$$

Equation (2.32) is linearized with respect to $\dot{\delta \bar{r}}$ and $\delta \bar{r}$. The resulting expressions for $\dot{\delta \bar{r}}$ and $\delta \bar{r}$ are

$$\dot{\delta r} = \frac{J - J_c}{[(\bar{n}_p \cdot \bar{A}) + \frac{1}{2} (\bar{n}_c \cdot \bar{B})(\Delta t)]} \quad (2.35a)$$

$$\delta r = \frac{1}{2} \frac{(J - J_c)\Delta t}{[(\bar{n}_p \cdot \bar{A}) + \frac{1}{2} (\bar{n}_c \cdot \bar{B})(\Delta t)]} \quad (2.35b)$$

with $\bar{A} \equiv \frac{\dot{r}}{r}$ (2.36)

$$\bar{B} \equiv \{(\bar{\omega} \times \bar{r}) - [\omega^2 - (\bar{\omega} \cdot \bar{n}_c)]\bar{r} + (1 - \mu)\bar{r}_1/r_1^3 + \mu\bar{r}_2/r_2^3\} \quad (2.37)$$

After the corrections $\delta \bar{r}$ and $\dot{\delta r}$ are made to the trajectory, the process is repeated until the desired stopping condition (perilune) is satisfied.

The method is applied to the circular restricted problem of three bodies, the elliptic restricted problem of three bodies and the ephemeral restricted problem of three bodies in Chapters 3, 4, and 5. The appropriate assumptions and modified equations will be presented in the appropriate chapters.

CHAPTER 3

CIRCULAR RESTRICTED PROBLEM OF THREE BODIES

For the planar circular restricted problem of three bodies, the motion of the massless particle takes place in the plane of motion of the two primaries and the primaries are each in circular orbits about their center of mass. This leads to the following reduced equations.

3.1 Equations for the Circular Restricted Problem of Three Bodies

The equation of motion is the same as Equation (2.1), and

$$\bar{R}_{2/1} = \bar{e}_x \quad ; \quad \dot{\bar{R}}_{2/1} = \bar{e}_y \quad ; \quad R_{2/1} = 1 \quad \text{and} \quad \dot{R}_{2/1} = 0 \quad (3.1)$$

which implies that

$$\bar{R}_1 = -\mu\bar{e}_x \quad , \quad \bar{R}_2 = (1 - \mu)\bar{e}_x \quad (3.2)$$

The out-of-plane component $z = 0$, and

$$\bar{\omega} = \bar{e}_z \quad , \quad \dot{\bar{\omega}} = 0 \quad (3.3)$$

The Jacobian function, J , [Equation (2.16)] remains the same, but the time rate of change of the Jacobian function, \dot{J} [Equation (2.17)], is zero.

The direction of the perturbing acceleration becomes

$$\bar{n}_p = \frac{-(\bar{e}_x + \bar{r}_2/r_2^3)}{|\bar{e}_x + \bar{r}_2/r_2^3|} \quad (3.4)$$

for motion relative to primary one. For motion relative to primary two, the direction of the perturbing acceleration is

$$\bar{n}_p = \frac{-(-\bar{e}_x + \bar{r}_1/r_1^3)}{|-\bar{e}_x + \bar{r}_1/r_1^3|} \quad (3.5)$$

The interval of propagation for the independent variable r_i ($i = 1,2$) is the same as Equation (2.25). Since the Jacobian function is a constant, the trapezoidal integration [Equation (2.26)] is not used. The linearized equations for δr and $\delta \dot{r}$ are the same as Equations (2.35a), and (2.35b) with the exception that

$$\bar{B} = \bar{e}_z \times \bar{r} - \bar{r} + (1 - \mu)\bar{r}_1/r_1^3 + \mu\bar{r}_2/r_2^3 \quad (3.6)$$

3.2 Velocity Correction Direction \bar{n}_p

The velocity is corrected in the time-averaged direction of the perturbing acceleration over the propagation interval. Since the independent variable is not time but is the position vector magnitude, this direction is approximated.

Figure 3.1 shows the variation of mean anomaly with the position vector magnitude for elliptic and hyperbolic conic orbits. Since the change in mean anomaly M is proportional to the change in time, these curves can be used to approximately determine the fraction of Δr corresponding to $\Delta t/2$.

Except near perifocus, the slopes of the curves shown in Figure 3.1 increase with increasing r . However, this increase is less for hyperbolic orbits than for elliptic orbits (see Figure 3.1). The average direction of the perturbing acceleration is approximated by choosing the positions of the non-primary force center and the massless particle to the following: on the Earth side of the mean surface of influence, their positions at the correction point are used; on the Moon side, the position of the Earth $2\Delta t/3$

before the correction point and the position of the massless body $2\Delta r/3$ before the correction point are used.

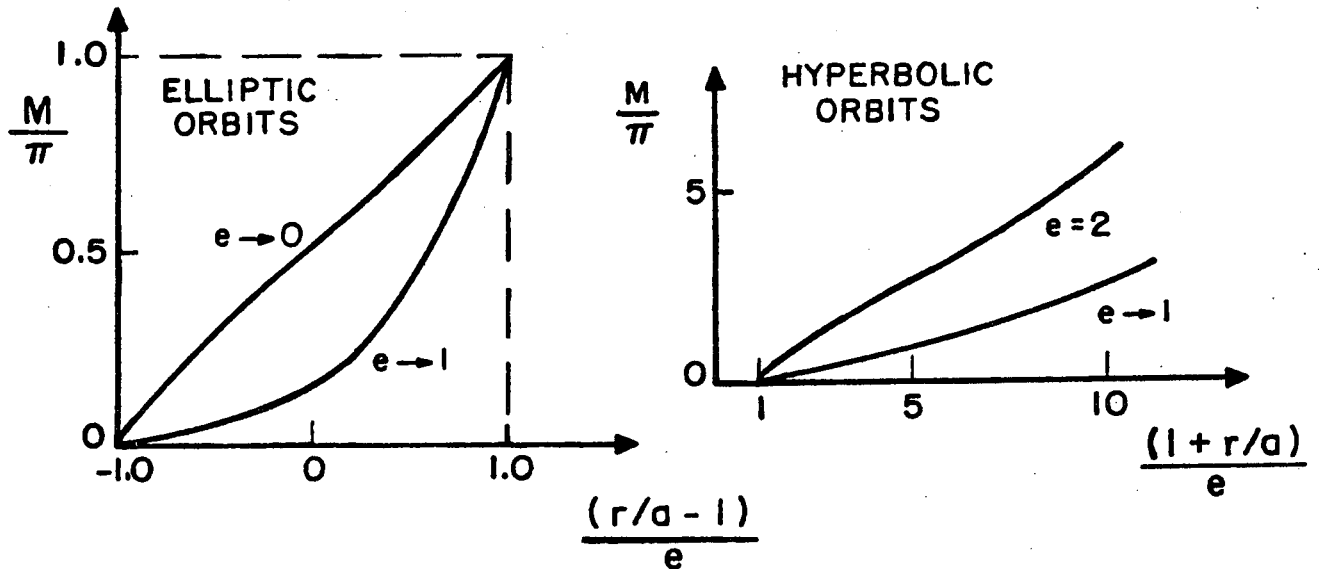


Figure 3.1 The Variation of Mean Anomaly and Position Vector Magnitude

3.3 Position Correction Direction \bar{n}_c

Two ways of calculating \bar{n}_c have been used. The first method uses the polar coordinates referenced to \bar{e}_x which are used to describe \bar{r}_1 , $\dot{\bar{r}}_1$, \bar{r}_2 , and $\dot{\bar{r}}_2$ (see Figure 3.2). In terms of the base vectors associated with these coordinate systems, the expression for \bar{n}_c is

$$\bar{n}_c = \bar{e}_r \cos \phi + \bar{e}_\alpha \sin \phi \tag{3.7}$$

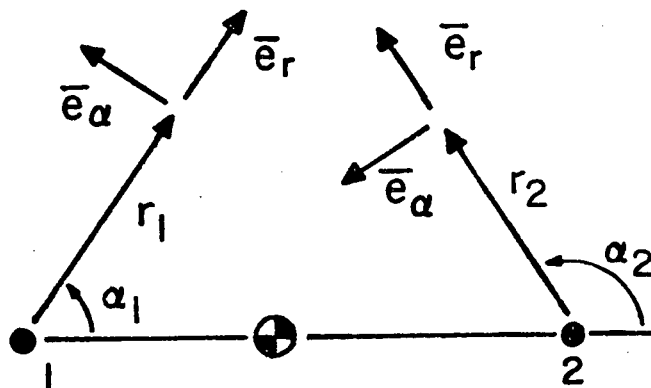


Figure 3.2 Polar Coordinate Systems

where ϕ is an angle measured positive counter-clock-wise from \bar{e}_r . This method of choosing \bar{n}_c is called the "refined method", because ϕ can be varied to give accurate results [see Table 1]. The variation of ϕ with perilune altitude is shown in Figure 3.3.

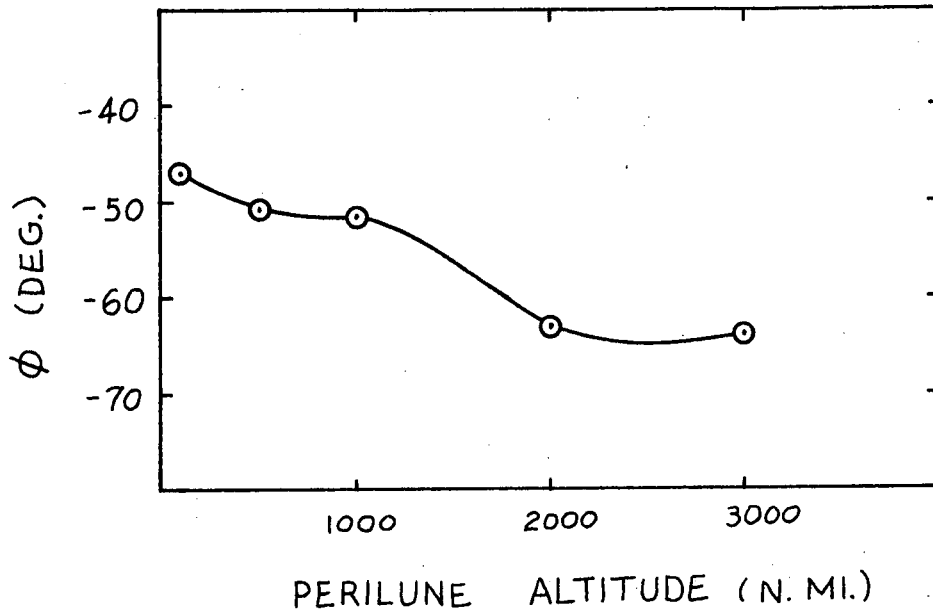


Figure 3.3 The Variation of ϕ With Perilune Altitude for the Circular Restricted Problem of Three Bodies

3.4 Numerical Results for "Refined" Choice of \bar{n}_c

In the non-dimensional system, the reference quantities are the following:

- | | | |
|------------------|---|---|
| reference mass | = | sum of the dimensional masses of the two primaries |
| reference length | = | dimensional distance between the two primaries
[60.2684 Earth radii (e_r) for the circular restricted problem of three bodies] |
| reference time | = | $[(\text{ref. length})^3 / G(\text{ref. mass})]^{1/2}$
= 104.21989489 hrs for the circular restricted problem of three bodies |

where G is the universal gravitational constant. The reference length was chosen as the average distance between the Earth and the Moon and the total mass of the Earth and the Moon. The masses of the Earth and Moon produced a mass-ratio parameter [Equation (2.2)] of $\mu = .012150446995297$.

The only fixed initial condition is

$$r_1 = .0173014 \quad (= 147 \text{ n. mi altitude}) \quad (3.8)$$

The initial value of the angle α_1 (see Figure 3.2) and the velocity components \dot{r}_1 and $r_1 \dot{\theta}_1$ are varied in order to attain different perilune altitudes. On the Earth side of the mean surface of influence

$$\begin{aligned} \Delta r_o &= .4977476 \quad (= 30 \text{ er}) \\ \Delta r_f &= .01659244 \quad (= 1.0 \text{ er}) \\ r_o &= .0173014 \quad (= 147 \text{ n. mi}) \end{aligned} \quad (3.9)$$

(r_f varies as the trajectory changes).

For the Moon side of the mean surface of influence,

$$\begin{aligned} \Delta r_o &= -.01659244 \quad (= -1.0 \text{ er}) \\ \Delta r_f &= -.03318488 \quad (= -2.0 \text{ er}) \\ r_o &= .1659244 \quad (= 10.0 \text{ er}) \\ r_f &= .00481180 \quad (= .29 \text{ er}) \end{aligned} \quad (3.10)$$

The values of r_2 , α_2 , $r_2 \dot{\theta}_2$ and time at perilune are compared with the integrated results, obtained with a Fehlberg^[10] Runge-Kutta RK 7(8), and with the patched-conic values. All runs were made on the CDC 6600 digital computer at the Computation Center of The University of Texas at Austin.

Execution times for this method are 0.32 seconds per run compared

to 2.0 seconds for the integrated trajectory and 0.12 seconds for the patched conic method.

Table 1. Numerical Results at Perilune for "Refined" Choice of \bar{n}_c
for the Circular Restricted Problem of Three Bodies

A. 73n. mi perilune altitude ($\phi = -47.164^\circ$)

	r_2	α_2 (rad)	$r_2 \dot{\theta}_2$	<u>time (hr)</u>
1) Integrated results	.0048727	.00476	-2.47678	68.703
2) "Jacobi" method	.0048760	.00903	-2.47603	68.641
Difference between (2) and (1)	.066% (.67n. mi)	.00427 (.245°)	+ .031% (+2.55fps)	-.062
3) Patched Conic Method	.0057996	.03138	-2.28714	69.773
Difference between (3) and (1)	19.0% (192.37n. mi)	.02662 (1.527°)	+7.656% (+637.5fps)	1.069

B. 501n. mi perilune altitude ($\phi = -50.658$)

1) Integrated	.0069359	.000155	-2.12414	73.182
2) "Jacobi"	.0069360	.000292	-2.12400	73.119
Difference (.0175n. mi)	.001% (.0175n. mi)	.000137 (.008°)	+ .006% (+ .459fps)	-.063
3) Patched Conic	.00839063	.032806	-1.95088	74.425
Difference (302n. mi)	20.97% (302n. mi)	.03566 (2.042°)	+8.156% (+582fps)	1.244

C. 1009n. mi perilune altitude ($\phi = -51.487^\circ$)

			$r_2 \dot{\theta}_2$	
1) Integrated	.0093806	.0000007	-1.872641	77.165
2) "Jacobi"	.0093802	-.0019233	-1.872487	77.107
Difference (-.0919n. mi)	-.005% (-.0919n. mi)	-.00193 (-.111°)	+ .008% (+.52fps)	-.058
3) Patched Conic	.01048787	-.006722	-1.764465	78.701
Difference (229.8n. mi)	11.80% (229.8n. mi)	-.006730 (-.386°)	+5.78% (+363.6fps)	1.535

D. 2000n. mi perilune altitude ($\phi = -63.039$)

	$\underline{r_2}$	$\underline{\alpha_2}$ (rad)	$\underline{r_2 \dot{\theta}_2}$	<u>time (hr)</u>
1) Integrated	.01415734	.0000012	-1.592244	83.116
2) "Jacobi"	.01416068	.0011052	-1.591828	83.007
Difference	.021%	.0011039	+ .026%	-.108
	(.608n. mi)	(.063°)	(+1.40fps)	
3) Patched Conic	.01608699	-.000542	-1.489750	84.881
Difference	13.63%	-.00054340	+6.437%	1.766
	(400.5n. mi)	(-.031°)	(+344.5fps)	1.766

E. 2995n. mi perilune altitude ($\phi = -63.395$)

1) Integrated	.0189500	.0000002	-1.431530	87.755
2) "Jacobi"	.0189542	-.0011399	-1.431254	87.654
Difference	.022%	-.0011401	+ .0193%	-.101
	(.833n. mi)	(-.065°)	(+ .929fps)	
3) Patched Conic	.0261182	-.0294720	-1.347823	89.894
Difference	8.77%	-.0294721	+5.85%	2.140
	(344.9n. mi)	(-1.690°)	(+281.4fps)	

3.5 Numerical Results for the "straight-forward" Choice of \bar{n}_c

For the "straight-forward" choice of \bar{n}_c is

$$\bar{n}_c = \sigma \bar{n}_p \quad (3.11)$$

where $\sigma = +1$ for the Earth side of the mean surface of influence, and $\sigma = -1$ for the Moon side of the mean surface of influence. This choice of \bar{n}_c will be discussed in Chapter 6. The only other difference between the two choices of \bar{n}_c is that on the Moon side of the surface of influence the position of primary one is Δt before the correction point instead of $\frac{2}{3} \Delta t$ and the position of the massless particle is Δr instead of $\frac{2}{3} \Delta r$. This is due to the fact that for the Earth side of the mean surface of influence the direction of the perturbing acceleration \bar{n}_p [Equation (3.4)] is almost in the direction of the perturbing body. But for the Moon side of the mean surface of influence, the direction of the perturbing acceleration \bar{n}_p [Equation (3.5)] leads the perturbing body by a significant amount. Therefore, it is more reasonable to use the position of the primary one at Δt instead of $\frac{2}{3} \Delta t$ before the correction point.

The numerical results for the straight-forward choice of \bar{n}_c are presented in Table 2. As shown in Table 2 the errors between the "straight-forward" choice of \bar{n}_c and the integrated results are all less than 10 n. mi and 10 fps. Execution times for the choice of \bar{n}_c are about the same as for the "refined" choice of \bar{n}_c . Therefore, it would seem logical to use the "straight forward" choice of \bar{n}_c as it does not change with perilune altitude.

Table 2. Numerical Results at Perilune for the "Straight-Forward" Choice of \bar{n}_c
 For the Circular Restricted Problem of Three Bodies

A. 73n. mi Perilune altitude

	r_2	α_2 (rad)	$r_2 \dot{\theta}_2$	Time (hr)
1) Integrated	.0048727	.004760	-2.47678	68.703
2) "Jacobi"	.0048615	.004150	-2.47902	68.635
Difference	-.231%	-.000615	.091%	-.068
	(-2.33n.mi)	(-.352°)	(7.54fps)	
3) Patched Conic	.00579909	.031340	-2.28722	69.773
Difference	19.0%	.026577	-7.65%	1.069
	(192.26n. mi)	(1.537°)	(637.2fps)	

B. 50ln. mi perilune altitude

1) Integrated	.0069359	.000155	-2.12414	73.182
2) "Jacobi"	.00693658	.000668	-2.12396	73.108
Difference	.0092%	.000514	-.0086%	-.073
	(.133n. mi)	(.029°)	(-.612fps)	
3) Patched Conic	.0083900	.03272	-1.95101	74.425
Difference	20.95%	.032566	-8.15%	1.244
	(301.6n. mi)	(1.866°)	(-581.9fps)	

C. 1009n. mi perilune altitude

1) Integrated	.0093806	.0000007	-1.872641	77.165
2) "Jacobi"	.0094122	.0009836	-1.870040	77.102
Difference	.337%	.0009829	-.139%	-.0638
	(6.56n. mi)	(.029°)	(-8.74fps)	
3) Patched Conic	.0111126	.0221121	-1.73254	78.604
Difference	18.46%	.022105	-7.481%	1.439
	(359.5n. mi)	(1.268°)	(-470.9fps)	

D. 2000n. mi perilune altitude

	$\underline{r_2}$	$\underline{\alpha_2}$ (rad)	$\underline{r_2 \dot{\theta}_2}$	<u>Time (hr)</u>
1) Integrated	.0141573	.0000001	-1.592244	83.116
2) "Jacobi"	.0141342	-.0010344	-1.592638	83.050
Difference	-.163% (-4.80n. mi)	-.0010349 (.059°)	.025% (1.32fps)	-.066
3) Patched Conic	.0161907	.0028447	-1.487178	84.867
Difference	14.4% (422.1n. mi)	.0028441 (.163°)	-6.599% (-353.2fps)	1.752

E. 2995n. mi perilune altitude

1) Integrated	.0189500	.0000002	-1.431530	87.755
2) "Jacobi"	.0189249	-.0010122	-1.431878	87.771
Difference	-.132% (-5.19n. mi)	-.0010124 (-.058°)	.024% (1.167fps)	-.043
3) Patched Conic	.0210521	-.0147625	-1.343576	89.782
Difference	11.09% (436.3n. mi)	-.0147627 (-.845°)	-6.144% (-295.6fps)	2.027

CHAPTER 4

ELLIPTIC RESTRICTED PROBLEM OF THREE BODIES

For the planar elliptic restricted problem of three bodies the motion is still in the (\bar{e}_x, \bar{e}_y) -plane. The only difference between the models for the circular restricted problem of three bodies and the elliptic restricted problem of three bodies is that the primaries are each in elliptic orbits about the CM. The choice of the eccentricity of the elliptic orbits is .0549, which is the average eccentricity of the Moon with respect to the Earth^[21]. The inclusion of the eccentricity of the primaries leads to the following equations.

4.1 Equations for the Elliptic Restricted Problem of Three Bodies

The equations of motion is the same as Equation (2.1), and

$$\bar{R}_{2/1} = R_{2/1} \bar{e}_x \quad , \quad \dot{\bar{R}}_{2/1} = \dot{R}_{2/1} \bar{e}_x + R_{2/1} \omega \bar{e}_y \quad (4.1)$$

$$R_{2/1} = 1 - e_{2/1} \cos E_{2/1} \quad ; \quad \dot{R}_{2/1} = e_{2/1} \sin E_{2/1} / R_{2/1} \quad (4.2)$$

where $e_{2/1}$ = the eccentricity of primary 2 relative to primary 1
 = .0549

$E_{2/1}$ = the eccentric anomaly of primary 2 relative to primary 1,
 which is obtained from solution of Kepler's Equation

$$0 \leq E_{2/1} \leq 2\pi$$

$$\begin{aligned} \omega &= \text{angular rate of primary 2 relative to primary 1} \\ &= \dot{f}_{2/1} = (1 - e_{2/1}^2)^{1/2} / R_{2/1}^2 \end{aligned} \quad (4.3)$$

$$\bar{R}_1 = -\mu R_{2/1} \bar{e}_x \quad ; \quad \bar{R}_2 = (1 - \mu) R_{2/1} \bar{e}_x \quad (4.4)$$

$$\bar{\omega} = \omega \bar{e}_z \quad ; \quad \dot{\bar{\omega}} = \dot{\omega} \bar{e}_z \quad (4.5)$$

where

$$\dot{\omega} = \ddot{f}_{2/1} = \frac{-2\dot{R}_{2/1}}{R_{2/1}} \dot{f}_{2/1} = -2\omega \frac{\dot{R}_{2/1}}{R_{2/1}} \quad (4.6)$$

The Jacobian function J [Equation (2.16)] remains the same, but the time rate of change of the Jacobian function, \dot{J} , [Equation (2.17)] becomes

$$\dot{J} = -\dot{\omega} \cdot \bar{h} + \mu(1 - \mu) \bar{R}_{2/1}^0 \cdot \left(\frac{\bar{r}_1}{r_1^3} - \frac{\bar{r}_2}{r_2^3} \right) \quad (4.7)$$

where

$$\bar{h} = \bar{r} \times \dot{\bar{r}} = \bar{r} \times \frac{0}{\bar{r}} + \bar{\omega} r^2 \quad (4.8)$$

The term $\bar{r}(\bar{\omega} \cdot \bar{r}) = 0$ since $\bar{\omega}$ is perpendicular to \bar{r} for the planar model. The direction of the perturbing acceleration becomes

$$\bar{n}_p = \frac{- (\bar{e}_x/R_{2/1}^2 + \bar{r}_2/r_2^3)}{|\bar{e}_x/R_{2/1}^2 + \bar{r}_2/r_2^3|} \quad (4.9)$$

for motion relative to primary 1. For motion relative to primary 2, the direction of the perturbing acceleration is

$$\bar{n}_p = \frac{- (-\bar{e}_x/R_{2/1}^2 + \bar{r}_1/r_1^3)}{|-\bar{e}_x/R_{2/1}^2 + \bar{r}_1/r_1^3|} \quad (4.10)$$

The interval of motion for r is the same as Equation (2.25). Since the Jacobian function is not constant ($\dot{J} \neq 0$) the trapezoidal integration [Equation (2.26)] is used to predict the proper value for the Jacobian function at the end of the interval of motion. The linearized equations for δr and $\delta \dot{r}$ are the same as Equations (2.35a) and (2.35b) except that

$$\bar{B} \equiv \{(\bar{\omega} \times \bar{r}) - \omega^2 \bar{r} + (1 - \mu) \frac{\bar{r}_1}{r_1} + \mu \frac{\bar{r}_2}{r_2}\} \quad (4.11)$$

The velocity and position correction directions are the same as described in Sections (3.2) and (3.3). The variation of ϕ [Equation (3.7)] with perilune altitude for the "refined" choice of \bar{n}_c shown in Figure 4.1

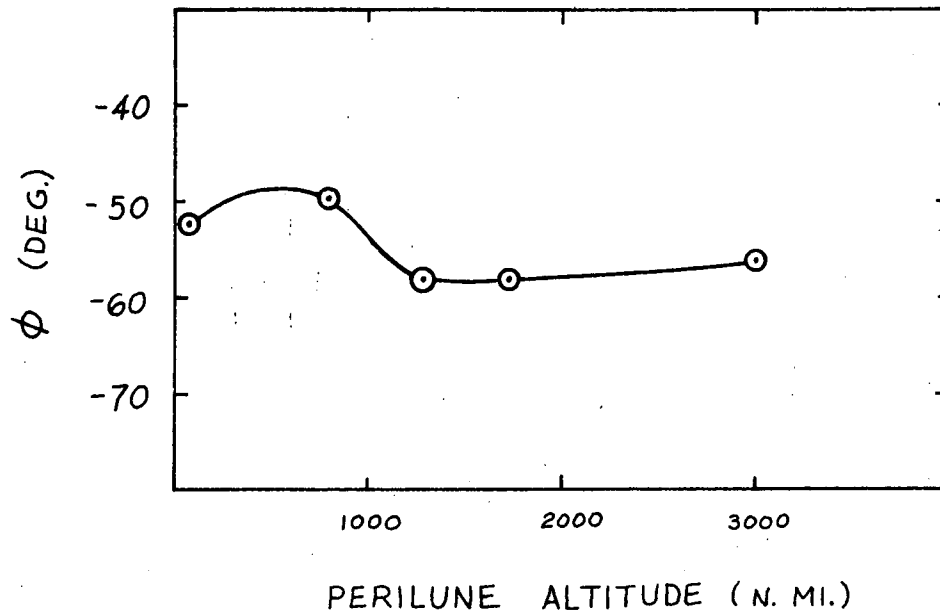


Figure 4.1 The Variation of ϕ With Perilune Altitude for the Elliptic Restricted Problem of Three Bodies

For the "straight-forward" method \bar{n}_c was calculated as presented in Equation (3.11).

4.2 Numerical Results for "Refined" and "Straight-Forward" Choice of \bar{n}_c .

The non-dimensional quantities for the elliptic restricted problem of three bodies are the same as those described in Section (3.4) with the exception that the reference length is the dimensional semi-major axis of

primary 2 relative to primary 1 (= 60.2684 er). The remaining initial conditions are as presented in Section (3.8).

The values of r_2 , α_2 , $r_2 \dot{\theta}_2$ and time at perilune for the "refined" and "straight-forward" methods are compared with the numerically integrated results and with the patched conic and are presented in Table 3.

Execution times for this problem are of the same order of magnitude as for the circular restricted problem of three bodies. That is, the Jacobian method takes about 0.3 seconds as compared with 2.0 seconds for the integrated trajectory and 0.13 seconds for the patched conic method.

Table 3. Numerical Results at Perilune For

Jacobi - 1 "Refined" Choice of \bar{n}_c

and

Jacobi - 2 - "Straight-Forward" Choice of \bar{n}_c A. 59.2n. mi Perilune Altitude

	r_2	α_2 (rad)	$r_2 \dot{\theta}_2$	time (hr)
1) Integrated Results	.00480695	-.15507493	-2.463639	69.084
2) Jacobi - 1($\phi = 52.2^\circ$)	.00480630	-.15516424	-2.463483	68.985
Difference between (1) and (2)	-.013% (-.134n. mi)	-.000089 (-.005°)	.006% (.525fps)	-.099
3) Jacobi - 2	.00480564	-.15456276	-2.461228	69.006
Difference between (a) and (3)	.028% (-.275n. mi)	.00050095 (.029°)	(- .097%) (-8.08fps)	-.078
4) Patched Conic	.00527354	-.15991492	-2.340174	70.458
Difference between (1) and (4)	9.71% (96.85n. mi)	-.00483401 (.277°)	5.01% (451.01fps)	1.374

B. 780.5n. mi Perilune Altitude

1) Integrated	.00828199	-.00361027	-1.9844195	69.951
2) Jacobi - 1($\phi = -49.8^\circ$)	.00828722	-.00746075	-1.9845066	69.846
Difference	.063% (1.085n. mi)	-.00385048 (-.222°)	-.004% (- .293fps)	-.105
3) Jacobi - 2	.00828288	.00589730	-1.9846983	69.829
Difference	.011% (.184n. mi)	.00870000 (.500°)	-.014% (- .937fps)	-.122
4) Patched Conic	.00876841	-.02646631	-1.8997533	71.458
Difference	5.87% (100.96n. mi)	-.02285604 (1.310°)	4.27% (284.59fps)	1.507

C. 1293.3n. mi Perilune Altitude

	r_2	α_2 (rad)	$r_2 \dot{\theta}_2$	<u>time (hr)</u>
1) Integrated	.01075232	.06710700	-1.8047416	70.518
2) Jacobi - 1($\phi = -58.0^\circ$)	.01075021	.07082385	-1.804806	70.407
Difference	-.020% (-.438n. mi)	.00371684 (.212°)	-.004% (-.219fps)	-.111
3) Jacobi - 2	.01071372	.07030673	-1.8069572	70.406
Difference	(-.359%) (-8.01n. mi)	.003199731 (.183°)	.122% (7.45cps)	-.112
4) Patched Conic	.01144598	.04941106	-1.7204624	72.039
Difference	6.45% (143.98n. mi)	-.01769594 (-.995%)	4.67% (283.29fps)	1.521

D. 1726.9n. mi Perilune Altitude

1) Integrated	.01284166	.11309066	-1.6982265	70.978
2) Jacobi - 1($\phi = -57.9^\circ$)	.01284165	.11658178	-1.6983320	70.846
Difference	-.000% (-.001n. mi)	.00349172 (.200°)	-.006% (.355fps)	-.132
3) Jacobi - 2	.01283529	.12227265	-1.6984975	70.859
Difference	-.050% (-1.32n. mi)	.00918228 (.526°)	-.016 (-.911fps)	-.119
4) Patched Conic	.01371698	.09959157	-1.6148834	72.509
Difference	6.82% (181.68n. mi)	-.01349849 (-.773°)	4.91% (280.15fps)	1.531

E. 3000.3n. mi Perilune Altitude

1) Integrated	.01897652	.20480733	-1.5023960	72.271
2) Jacobi - 1($\phi = -55.8^\circ$)	.01897642	.20418418	-1.5023960	72.135
Difference	.016% (.648n. mi)	-.00062315 (-.036°)	.020% (1.03fps)	-.136
3) Jacobi - 2	.01901113	.21273488	-1.4997524	72.161
Difference	.182% (7.19n. mi)	.00792754 (.046°)	.176% (8.89fps)	-.110
4) Patched Conic	.02022279	.19094782	-1.4176655	73.945
Difference	6.57% (258.68n. mi)	-.01385952 (-.795°)	5.64% (284.81fps)	1.674

For the "refined" method the errors between the Jacobian method and the numerically integrated results are less than 1.1 n. mi and 1.1 fps. For the "straight-forward" method the errors at perilune are all less than 10 n. mi and 10 fps.

CHAPTER 5

EPHEMERAL RESTRICTED PROBLEM OF THREE BODIES

For the ephemeral restricted problem of three bodies the motion of the massless particle is not constrained to be planar and motion of the primaries is not two-body motion about the center of mass. The position and velocity of the primaries are taken from the JPL ephemeris tape^[6] at each point of interest. This leads to the following equations.

5.1 Equations for the Ephemeral Restricted Problem of Three Bodies

The non-dimensional equation of motion for the massless particle is the same as Equation (2.1), and

$$\bar{\mathbf{R}}_{2/1} = R_{2/1} \bar{\mathbf{e}}_x \quad ; \quad \dot{\bar{\mathbf{R}}}_{2/1} = \dot{R}_{2/1} \bar{\mathbf{e}}_x + R_{2/1} \dot{f}_{2/1} \bar{\mathbf{e}}_y \quad (5.1)$$

where $\bar{\mathbf{R}}_{2/1}$ and $\dot{\bar{\mathbf{R}}}_{2/1}$ are taken from the ephemeris tape. The angular velocity and acceleration of the primaries relative to the CM is determined by

$$\bar{\boldsymbol{\omega}} = \omega \bar{\mathbf{e}}_z = \dot{f}_{2/1} \bar{\mathbf{e}}_z = \frac{\bar{\mathbf{R}}_{2/1} \times \dot{\bar{\mathbf{R}}}_{2/1}}{R_{2/1}^2} \quad (5.2)$$

$$\dot{\bar{\boldsymbol{\omega}}} = \dot{\omega} \bar{\mathbf{e}}_z = \ddot{f}_{2/1} \bar{\mathbf{e}}_z = \frac{\bar{\mathbf{R}}_{2/1} \times \ddot{\bar{\mathbf{R}}}_{2/1}}{R_{2/1}^2} - \frac{2\dot{R}_{2/1}}{R_{2/1}^3} (\bar{\mathbf{R}}_{2/1} \times \dot{\bar{\mathbf{R}}}_{2/1}) \quad (5.3)$$

Since the acceleration $\ddot{\bar{\mathbf{R}}}_{2/1}$ is not given, and is not easily calculated, it is assumed that at each instant in time that

$$\ddot{\bar{\mathbf{R}}}_{2/1} = - \frac{\bar{\mathbf{R}}_{2/1}}{R_{2/1}^3} \quad (5.4)$$

therefore,

$$\dot{\omega} = -2\omega \frac{\dot{R}_{2/1}}{R_{2/1}} \quad (5.5)$$

The out-of-plane components, z and \dot{z} , are not necessarily zero for the ephemeral restricted problem of three bodies.

The Jacobian function J and the time rate of change of the Jacobian function \dot{J} remain the same as Equation (2.16) and (2.17) respectively. The direction of the perturbing acceleration for motion relative to primary one and primary two remains the same as Equations (2.23) and (2.24) respectively.

The interval of motion for the independent variable r is the same as Equation (2.25). The estimate value of the Jacobian function, J , at the end of an interval of motion is predicted using Equation (2.26). The linearized equations for $\delta\dot{r}$ and δr are the same as Equations (2.35a) and (2.35b), where \bar{A} and \bar{B} are defined in Equations (2.36) and (2.37).

For the circular and elliptic restricted problems of three bodies the results were presented for a "refined" choice of \bar{n}_c , and for a "straight-forward" choice of \bar{n}_c . Since the results for the "straight-forward" choice of \bar{n}_c were quite satisfactory, it was decided to only present the results for the "straight-forward" choice of \bar{n}_c for the ephemeral restricted problem of three bodies.

5.2 Velocity Correction Direction \bar{n}_p

The velocity is corrected in the time-averaged direction of the perturbing acceleration over the propagation interval. Since the independent variable is not time but is the position vector magnitude, this direction is approximated by choosing the positions of the non-primary force center and the massless particle to be the following: on the Earth side of the mean

surface of influence, their positions at the correction are used; on the Moon side, the position of the Earth Δt before the correction point and the position of the massless body Δr before the correction point are used. The unit vector \bar{n}_p is the direction from the massless body in the direction of the perturbing acceleration. The reason for this choice of positions of the bodies for computing \bar{n}_p rather than the choice used in Section (3.2) is not entirely obvious. For motion relative to primary one the direction of the perturbing acceleration is in the approximate direction of the perturbing body. Thus, it is logical to use the position of the massless particle and perturbing body at the time and position of the correction. For motion relative to primary two the direction of the perturbing acceleration leads the direction of the perturbing body. This coupled with the "straight-forward" choice of \bar{n}_c lead to the choice of the position of massless particle and perturbing body described above.

5.3 Position Correction Direction \bar{n}_c

For the ephemeral restricted problem of three bodies only one choice of \bar{n}_c has been used. This is the "straight-forward" choice as described in Section (3.5). One advantage to this choice of \bar{n}_c is that it is not dependent upon the perilune altitude. An explanation of the reason the "straight-forward" choice of \bar{n}_c works is presented in Chapter 6.

5.4 Numerical Results for the Ephemeral Restricted Problem of Three Bodies

For the ephemeral restricted problem of three bodies the non-dimensionalizing reference quantities are the following:

reference mass = sum of dimensional masses of the two primaries
 reference length = semi-major axis of primary two relative to

primary one at the epoch time (April 11, 1970,

21^h 53^{min} 48.966^{sec})

= 59.6789353907 er

reference time = $[(\text{ref. length})^3 / G(\text{ref. mass})]^{1/2}$

= 102.694503141307 hrs

The mass of the Earth and Moon taken from the ephemeris tape^[6] produced a mass ratio parameter [Equation (2.2)] of $\mu = .01215052064981$.

The only fixed initial condition is

$r_1 = .01754507908$ (= 162.10n. mi altitude)

The remaining four initial conditions are varied to attain different perilune altitudes. The coordinate system used for the ephemeral restricted problem of three bodies is a cylindrical system measured from the instantaneous Earth-Moon plane and from the Earth-Moon line. See Figure 5.1.

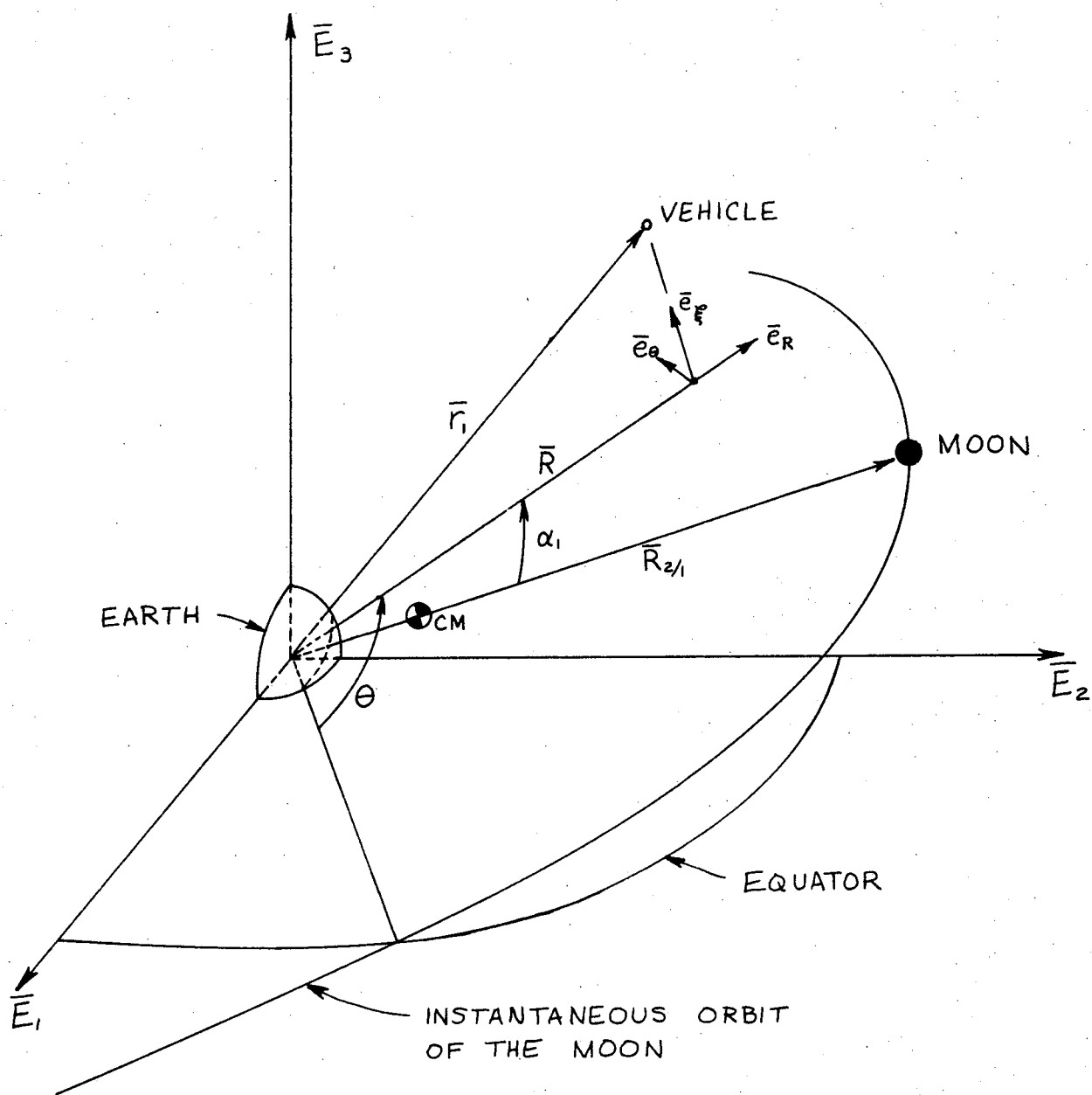


Figure 5.1 Cylindrical Coordinates Used in the Ephemeris Restricted Problem of Three Bodies

The following equations are true for the cylindrical coordinate system.

$$\bar{r}_1 = R_1 \bar{e}_{R_1} + z_1 \bar{e}_{\xi_1} \quad (5.7)$$

$$\dot{\bar{r}}_1 = \dot{R}_1 \bar{e}_{R_1} + R_1 \dot{\theta}_1 \bar{e}_{\theta_1} + \dot{z}_1 \bar{e}_{\xi_1} \quad (5.8)$$

where R_1 should not be confused with \bar{R}_1 measured from the CM to primary one. On the Earth side of the mean surface of influence

$$\Delta r_o = .4977476 \quad (= 30 \text{ er})$$

$$\Delta r_f = .01659244 \quad (= 1.0 \text{ er})$$

$$r_o = .017545079 \quad (= 162.1 \text{ n. mi})$$

(r_f varies as the trajectory changes).

For the Moon side of the mean surface of influence the values of Δr_o , Δr_f , r_o and r_f are the same as those presented in Section (3.4).

The values of α_2 , $R_2 \dot{\theta}_2$, $|\bar{r}_2|$ and $|\dot{\bar{r}}_2|$ and time at perilune are compared with the numerically integrated results obtained with the RK7(8) and with the patched conic and are presented in Table 4. The values for R_2 , z_2 , and \dot{z}_2 are not presented but compare well with the integrated results.

Execution times for this method are 0.47 seconds per run compared to 7.0 seconds for the integrated trajectory and 0.22 seconds for the patched conic method. The reason for the significant increase in execution time for the Jacobi method and the numerical integration is the extra time required to call the ephemeris tape at each step. The patched conic method only has to call the ephemeris tape three times per case.

Table 4. Numerical Results at Perilune for "Straight-Forward" Choice of \bar{n}_c for the
Ephemerical Restricted Problem of Three Bodies

A. 69.2n. mi Perilune Altitude

	α_2 (rad)	$R_2 \dot{\theta}_2$	$ \bar{r}_2 $	$ \dot{\bar{r}}_2 $	<u>Time (hr)</u>
1) Integrated	.0025196	-2.4383941	.00490270	2.4526046	73.185
2) Jacobi - 2	.0006733	-2.4368515	.00490240	2.4510451	73.304
Difference between (1) and (2)	-.0018463 (-.106°)	- .063% (5.21fps)	-.007% (-.07n. mi)	- .064% (-5.27fps)	+ .199
3) Patched Conic	.0508569	-2.2093458	.00614394	2.2192867	74.305
Difference between (1) and (2)	.0483373 (2.769°)	-9.39% (773.71fps)	25.32% (255.11n. mi)	-9.51% (-788.13fps)	+1.120

B. 198.5n. mi Perilune Altitude

1) Integrated	.03789431	-2.3234660	.00553223	2.3344527	73.312
2) Jacobi - 2	.03598942	-2.3218661	.00553144	2.3328465	73.433
Difference (-.109°)	-.00190490 (-.109°)	+ .437% (.291fps)	-.014% (-.164n. mi)	-.068% (-5.43fps)	+ .121
3) Patched Conic	.08310205	-2.1174711	.006848689	2.1253222	74.435
Difference (2.590°)	.0452077 (2.590°)	8.87% (695.8fps)	23.80% (270.57n. mi)	-8.96% (-706.4fps)	+1.123

C. 488.8n. mi Perilune Altitude

	α_2 (rad)	$R_2 \dot{\theta}_2$	$ \bar{r}_2 $	$ \dot{r}_2 $	Time (hr)
1) Integrated	.10475594	-2.1270724	.00694462	2.1337672	73.584
2) Jacobi - 2	.10307331	-2.1271008	.00692813	2.1338228	73.707
Difference	-.0016826 (-.096°)	-.001% (-.096fps)	-.237% (-3.39n. mi)	.003% (.188fps)	+ .122
3) Patched Conic	.13507698	-1.9714833	.00824681	1.9766647	74.737
Difference	.0303210 (1.737°)	+7.315% (525.57fps)	18.75% (267.64n. mi)	-7.36% (-530.68fps)	+1.153

D. 975.6n. mi Perilune Altitude

1) Integrated	.18567690	-1.9091071	.00931305	1.9104482	74.262
2) Jacobi - 2	.18454745	-1.9072579	.00930723	1.9086020	74.391
Difference	-.0011295 (.065°)	+ .097% (6.25fps)	-.062% (-1.20n. mi)	-.097% (-6.24fps)	+ .129
3) Patched Conic	.21112820	-1.7836686	.010864705	1.7847919	75.433
Difference	.0254513 (1.458°)	+6.57% (423.72fps)	16.66% (318.91n. mi)	-6.57% (-424.46fps)	+1.171

E. 2379.7n. mi Perilune Altitude

	α_2 (rad)	$R_2 \ddot{\theta}_2$	$ \bar{r}_2 $	$ \dot{\bar{r}}_2 $	Time (hr)
1) Integrated	.33873037	-1.5927180	.01614465	1.4937280	75.119
2) Jacobi - 2	.33598404	-1.5908406	.01610806	1.5918543	75.245
Difference	-.0027463 (-.157°)	+ .118% (6.34fps)	-.227% (-7.52n. mi)	+.118% (+6.33fps)	+ .126
3) Patched Conic	.34675503	-1.5131718	.017912635	1.5140690	76.346
Difference	.0080247 (.459°)	+4.99% (268.70fps)	10.95% (363.37n. mi)	+5.00% (+269.10fps)	+1.227 -1.227

F. 4550.9n. mi Perilune Altitude

1) Integrated	.45144918	-1.3871586	.026708638	1.3875241	76.669
2) Jacobi - 2	.45023525	-1.3840171	.026658933	1.3843824	76.812
Difference	-.0012139 (-.069°)	+ .226% (10.61fps)	-.186% (-10.22n. mi)	-.226% (-10.61fps)	+ .143
3) Patched Conic	.44829182	-1.3217430	.028746553	1.3220842	78.025
Difference	-.0031574 (-.181°)	+4.72% (220.97fps)	7.63% (418.85n. mi)	-4.72% (-221.05fps)	+1.356

Using the "straight-forward" choice of \bar{n}_c for the ephemeral restricted problem of three bodies, it is shown in Table 4 that Jacobi-2 correction method maintains the position and velocity errors to within 11 n. mi and 11 fps.

CHAPTER 6

DISCUSSION OF CHOICE OF CORRECTION DIRECTION

The choice of the velocity correction direction \bar{n}_p is straightforward and does not need much explanation. But, the "refined" choice, and the "straight-forward" choice of \bar{n}_c should be discussed in greater detail. To do this a little background history is in order.

6.1 Background History

When the Jacobian correction method was first conceived, it was believed that if the velocity were corrected back to the proper value often enough there would be no need for a position correction. This method was first applied to the circular restricted problem of three bodies and, with only one scalar function, it was thought that only one quantity could be corrected. The results of the Jacobian correction method evaluated at the terminal point were a 10% to 20% improvement over the patched conic method. These results were compared at the point in the trajectory where the force center was changed from primary one to primary two. At this patch point the Jacobian method appeared to be much superior to the patched conic. However, the results deteriorated rapidly from the patch point in toward primary two. It was then realized that all the position errors that had been neglected along the trajectory transformed into a velocity error after switching to primary two as the force center. This position and velocity error at the mean surface of influence then propagated into large errors in both position and velocity at the terminal point.

6.2 Logical Steps That Led to the Choice of \bar{n}_c

This resulted in the approximation that

$$\delta \dot{\bar{r}} = \bar{a} \Delta t \quad (6.1)$$

where \bar{a} is defined in Equation (2.33). Then,

$$\delta \bar{r} = \frac{1}{2} \bar{a} (\Delta t)^2 = \frac{1}{2} \delta \dot{\bar{r}} \Delta t \quad (6.2)$$

At this point, it was not clear whether \bar{n}_c would be equal to \bar{n}_p or not.

By ignoring the difference between \bar{n}_c and \bar{n}_p then,

$$\delta r = \frac{1}{2} \delta \dot{r} \Delta t \quad (6.3)$$

which is the relationship necessary to obtain two quantities from one scalar function (the Jacobian function). The corrections δr and $\delta \dot{r}$ [Equations (2.35a) and (2.35b)] were easily determined from the linearized form of Equation (2.32).

Since a relationship between \bar{n}_c and \bar{n}_p was not apparent, it was decided to vary the direction of \bar{n}_c through 360° . This led to the relationship that

$$\bar{n}_c = \bar{e}_r \cos \phi + \bar{e}_\alpha \sin \phi \quad (6.4)$$

as described in Section (3.3). From this assumption the results presented in Table 1 were generated. It was observed that, for motion relative to primary one, the angle between \bar{n}_p and \bar{n}_c was always within $\pm 10^\circ$ of zero and, for motion relative to primary two, the angle between \bar{n}_p and \bar{n}_c was very close to $\pm 180^\circ$. This seemed peculiar until the equations for \bar{n}_p [Equation (2.23) and (2.24)] were analyzed. From Equation (2.23)

$$\bar{n}_p = \frac{- (\bar{R}_{2/1}/R_{2/1}^3 + \bar{r}_2/r_2^3)}{|\bar{R}_{2/1}/R_{2/1}^3 + \bar{r}_2/r_2^3|} \quad (6.5)$$

in the interval as r_1 goes from .5 \rightarrow .9 and r_2 goes from .6 \rightarrow .2 it

is clear that

$$\bar{n}_p \approx \frac{-\bar{r}_2}{|\bar{r}_2|} \quad (6.6)$$

where

$$R_{2/1} = 1.0 \quad (6.7)$$

From Equation (2.24)

$$\bar{n}_p = \frac{-(-\bar{R}_{2/1}/R_{2/1}^3 + \bar{r}_1/r_1^3)}{|-\bar{R}_{2/1}/R_{2/1}^3 + \bar{r}_1/r_1^3|} \quad (6.8)$$

In the interval as r_1 goes from $.8 \rightarrow 1.02$ and r_2 goes from $.2 \rightarrow .02$ then

$$\bar{n}_p \neq \frac{-\bar{r}_1}{|\bar{r}_1|} \quad (6.9)$$

but \bar{n}_p points in front of primary one for all corrections.

It then seemed obvious to correct the position vector in the direction of \bar{n}_p going from primary one to the mean surface of influence and, for the motion from the mean surface of influence into primary two, in the opposite direction to \bar{n}_p .

$$\bar{n}_c = \begin{cases} +\bar{n}_p & \text{on primary one side} \\ -\bar{n}_p & \text{on primary two side} \end{cases} \quad (6.10)$$

The numerical results for the "straight-forward" choice of \bar{n}_c presented in Table 2 validated this choice of \bar{n}_c as being a good one.

When the same choice of \bar{n}_c was applied to the elliptic restricted problem of three bodies and the ephemerical restricted problem of three bodies, the results were within acceptable limits [Tables 3 and 4] and provided further evidence in favor of the "straight-forward" choice.

CHAPTER 7

COMPARISONS, CONCLUSIONS, AND RECOMMENDATIONS

7.1 Summary

An approximate solution to the restricted problem of three bodies has been presented in the previous chapters. The theory of the Jacobian correction method has been developed and the method has been applied to the circular, the elliptic, and the ephemeral restricted problems of three bodies with good results. Two methods of determining the position vector correction direction (\bar{n}_c) have been presented. The numerical results for both choices of \bar{n}_c have been presented for the circular and elliptic problems. Only the "straight-forward" choice of \bar{n}_c was used for the ephemeral restricted problem of three bodies. The results have indicated that the "straight-forward" choice of \bar{n}_c is more desirable, because it is independent of the perilune altitude. A qualitative comparison of methods and conclusions and recommendations are presented in this chapter.

7.2 Comparison of Methods

The purpose of this research has been to develop a method of generating approximate Earth-Moon or interplanetary trajectories using knowledge of functions which are constant or slowly-varying for the exact motion. This method is compared with the qualitative characteristics of each of the existing methods.

A comparison with the hybrid patched conic technique^[9] shows that the hybrid patched conic technique requires a patched conic trajectory as a reference trajectory. That is, a complete patched conic trajectory must be computed before the hybrid patched conic technique can be applied to the

trajectory. Although the Jacobian method use frequently corrected conic motion, a complete patched conic trajectory does not have to be calculated before the Jacobian method can be applied. The hybrid patched conic technique forms a curve fit to the perturbative accelerations, which is then analytically integrated to form corrections to the conic state vector. This technique works well for low perilune trajectories, but due to the nature of the curve fit breaks down for high perilune trajectories^[4]. The Jacobian method gives good results for trajectories that have various perilune altitudes (see Tables 1, 2, 3, and 4).

The multi-conic technique^[4] has the capability of including Earth oblateness terms plus the effect of any number of gravitational bodies. A simplified computational algorithm for the multi-conic as applied to the restricted problem of three bodies:

1. Advance conically in geocentric space from t to $t + \Delta t$.
2. Calculate the average perturbing acceleration due to the geocentric motion of the moon.
3. Modify the state vectors at the end of step 1 by

$$\Delta \bar{V} = \bar{a} \Delta t \quad (7.1)$$

$$\Delta \bar{R} = \frac{1}{2} \bar{a} \Delta t^2 \quad (7.2)$$

where \bar{a} = average perturbing acceleration .

4. Convert the corrected geocentric state to a selenocentric state which is then projected back in time along the straight line defined by the velocity vector an amount Δt . This is the trajectory in a "no gravity field".
5. The state is then advanced along a Moon-centered conic an

amount Δt from the "no gravity" state. The final vector transformed to geocentric coordinates defines the new Earth-centered conic.

6. The process is repeated using the new Earth-centered conic as the starting point.

The Jacobian method consists of a conically advanced state that is frequently corrected which is less complicated than the multi-conic. However, other perturbing bodies and Earth-oblateness terms have been incorporated into the multi-conic method. Neither have been used in the Jacobian method.

The pseudo-conic or the overlapped conic technique^[31] considers only the effects of the two primaries in the equation of motion and these only within a certain distance of the Moon (a "pseudo-sphere of about 24 r is defined). Farther from the Moon only pure Earth conic motion is used. The overlapped conic technique actually takes less computer time than the patched conic method and the Jacobian technique requires about 2 to 3 times as much computational time as the patched conic. However, the overlapped conic technique corrects only approximately 80% of the errors from the patched conic method.

A qualitative comparison between the Jacobian correction method and the matched asymptotic expansion technique^[11,12,13,14] indicates that the matched asymptotic expansion technique is an analytical approximation to the restricted problem of three bodies, and the Jacobian method is a numerical approximation. The Jacobian method is much easier to formulate and program than the matched asymptotic expansion technique.

7.3 Conclusions

The investigation described in the previous chapters has been concerned with developing a method of numerically predicting, as a function of

time, the position and velocity of a space vehicle in the restricted problem of three bodies utilizing knowledge of the constant or slowly-varying functions of the motion. It has been desirable for the method to be computationally fast and accurate as compared to numerical integrated trajectories and the patched conic trajectories. Numerical results indicate that the method provides a significant improvement over existing methods in the area of simplicity and is much more accurate than the patched conic method.

Based on the results presented previously in this report, the following conclusions can be drawn:

1. The procedure for implementing the Jacobian correction method is very simple and straight-forward.
2. The numerical results of the Jacobian correction method are a significant improvement over the patched conic and are accurate as compared to numerical integration.
3. The numerical results of the Jacobian method do not deteriorate for high perilune altitudes.
4. The method of handling the slowly-varying Jacobian function for the elliptic and ephemeral restricted problems is adequate for all cases presented.
5. The Jacobian correction method is sufficiently accurate to calculate trajectories with various perilune altitudes in the restricted problem of three bodies.
6. The "straight-forward" choice of \bar{n}_c , as presented in Chapters 4, 5, and 6, yields sufficiently accurate results and does not depend upon the perilune altitude.
7. The Jacobian correction method is computationally simple (and, therefore, fast) because it does not require a reference

trajectory, is not iterative, and needs no retracing.

7.4 Recommendations for Future Study

It is believed that further study in the following areas would be useful:

1. Implementation of oblateness effects when in the near vicinity of the primaries. It is recommended that the method developed by Penzo^[20] be used as the method of incorporating the oblateness effects.
2. Other perturbing bodies could be included. This would add terms to \dot{J} , if the value of J at the correction point could predict accurately enough, a procedure similar to the one presented in this report could be used.
3. Extending the method to free-return and interplanetary trajectories would also be quite useful.
4. It also would be useful to compare the method presented by Nacozy^[17] with this method to see how similar the correction directions are.

BIBLIOGRAPHY

1. Aarseth, S. J., "Dynamical Evolution of Clusters of Galaxies, II", Monthly Notices of The Royal Astronomical Society, Vol. 132, No. 1, pp. 35-65, 1966.
2. Battin, R. H., Astronautical Guidance, McGraw-Hill, 1964.
3. Brooks, J. E., "Formulation of the Equations of Motion, The Jacobi Condition, and Spheres of Action for Earth-Moon Vehicle Three-Body Systems", 9800.2-29, Space Technology Laboratories, 2 January 1963.
4. Byrnes, D. V. and Hooper, H. L., "Multi-Conic" A Fast and Accurate Method of Computing Space Flight Trajectories", AIAA Paper No. 70-1062, AAS/AIAA Astrodynamics Conference, Santa Barbara, California/ August 19-21, 1970.
5. Carlson, Neal Adrian, "An Explicit Analytic Guidance Formulation for Many-Body Space Trajectories", Massachusetts Institute of Technology TE-30, May 1969.
6. Devine, Charles J., "JPL Development Ephemeris Number 19", JPL Technical Report 32-1181, November 15, 1967.
7. Egorov, V. A., "Certain Problems of Moon Flight Dynamics", Russian Literature of Satellites, Part I, International Physical Index, 1958.
8. Escobal, P. R., Methods of Astrodynamics, John Wiley, 1968.
9. Escobal, P. R., Forster, K., Stern G. S. and Stern, R. J., "The Hybrid Patched Conic Technique as Applied to the Lunar Trajectory Problem", The Journal of the Astronautical Sciences, Vol. XVI, No. 3, pp. 97-109, May-June 1969.
10. Fehlberg, Erwin, "Classical Fifth-, Sixth-, Seventh-, and Eighth-Order Runge-Kutta Formulas with Stepsize Control", NASA TR R-287, October 1968.
11. Kevorkian, J. and Brachet, G., "Numerical Analysis of the Asymptotic Solution for Earth-to-Moon Trajectories", AIAA Journal, Vol. 7, No. 5, May 1969.
12. Lagerstrom, P. A. and Kevorkian, J., "Earth-to-Moon Trajectories in the Restricted Three-Body Problem", Journal de Mécanique, Vol. II, No. 2, June 1963.
13. Lagerstrom, P. A. and Kevorkian, J., "Earth-to-Moon Trajectories with Minimal Energy", Journal de Mécanique, Vol. II, No. 4, December 1963.
14. Lancaster, P. E. and Kevorkian, J., "Nonplanar Moon-to-Earth Trajectories", AIAA Journal, Vol. 6, No. 10, October 1968.

15. Miller, R. H., "Partial Iterative Refinements", Institute of Computer Research, The University of Chicago, Chicago, Illinois (undated).
16. Miller, R. H., "Irreversibility in Small Stellar Dynamical Systems", Astrophysical Journal, Vol. 140, No. 1, pp. 250-256, July 1 - November 15, 1964.
17. Nacozy, Paul E., "The Use of Integrals in Numerical Integrations of the N-Body Problem", Applied Mechanics Research Laboratory Report AMRL 1082, November 1970.
18. O'Handley, D. A., Holdridge, D. B., Melbourne, W. G. and Mulholland, J. D., "JPL Development Ephemeris Number 69", JPL Technical Report 32-1181, November 15, 1967.
19. Ovenden, M. W. and Roy A. E., "On the Use of the Jacobi Integral of the Restricted Three-Body Problem", Monthly Notices of the Royal Astronomical Society, Vol. 23, No. 1, 1961.
20. Penzo, Paul A., "Computing Earth Oblateness Effects on Lunar and Interplanetary Trajectories", AIAA Paper No. 70-97, January 1970.
21. Roy, Archie E., The Foundations of Astrodynamics, The Macmillan Company, New York, 1965.
22. Russell, P. E., "An Investigation of Three Possible Techniques for Improving the Analytic Lunar Program", TRW I.O.C. 3421.6-107, October 7, 1966.
23. Russell, P. E. and Culpepper, Bobby, "Calculation of Trajectories Utilizing Constant and/or Slowly Varying Functions", AIAA Paper No. 70-1076, AAS/AIAA Astrodynamics Conference, Santa Barbara, California, August 19-21, 1970.
24. Russell, P. E. and Culpepper, Bobby, "Calculation of Trajectories Utilizing A Slowly-Varying Jacobi Function", AAS Paper No. 71-381, AAS/AIAA Astrodynamics Specialists Conference, Ft. Lauderdale, Florida, August 17-19, 1971
25. Stern, R. J., Stern, G. S., Forester, K. and Escobal, P. R., "The Hybrid Patched Conic Applied to Lunar Return Trajectory Propagation", The Journal of the Astronautical Sciences, Vol. XVII, No. 1, pp. 25-43, July-August 1969.
26. Stumpff, K. and Weiss, E. H., "Application of an N-Body Reference Orbit", The Journal of the Astronautical Sciences, Vol. XV, No. 5, pp. 257-261, September-October 1968.
27. Suttles, T. E., "Calibration of Analytic Lunar Programs", TRW Systems Report 3832-6002-R4000, August 1965.
28. Suttles, T. E., "The Jacobi Condition in Analytic Lunar Simulations", undated TRW Systems Report.

29. Szebehely, Victor, Theory of Orbits, Academic Press, 1967.
30. Wilson, S. W., Jr., "A Pseudostate Theory for the Approximation of Three-Body Trajectories", TRW Note No. 69-FMT-765, August 15, 1969.
31. Wilson, S. W., Jr., "A Pseudostate Theory for the Approximation of Three-Body Trajectories", AIAA Paper No. 70-1061, August 1970.